Environmental Pollution 311 (2022) 119901

Contents lists available at ScienceDirect

Environmental Pollution

journal homepage: www.elsevier.com/locate/envpol

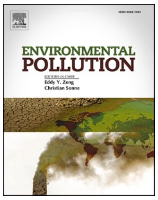

The role of physico-chemical interactions in the seasonality of toxic dinoflagellate cyst assemblages: The case of the NW Patagonian fjords system☆

Camilo Rodríguez–Villegas[a,b,c,*], Patricio A. Díaz[b,c], Pablo Salgado[d], Stephen J. Tomasetti[e], Manuel Díaz[f,g], Sandra L. Marín[g], Ángela M. Baldrich[a,b,c], Edwin Niklitschek[b], Loreto Pino[h], Thamara Matamala[h], Katherine Espinoza[h], Rosa I. Figueroa[i]

[a] *Programa de Doctorado en Ciencias, Mención Conservación y Manejo de Recursos Naturales, Universidad de Los Lagos, Camino Chinquihue Km 6, Puerto Montt, Chile*
[b] *Centro i~mar, Universidad de Los Lagos, Casilla 557, Puerto Montt, Chile*
[c] *CeBiB, Universidad de Los Lagos, Casilla 557, Puerto Montt, Chile*
[d] *Centro de Estudios de Algas Nocivas (CREAN), Instituto de Fomento Pesquero (IFOP), Enrique Abello 0552, Punta Arenas, Chile*
[e] *Environmental Studies Program, Hamilton College, Clinton, NY, USA*
[f] *Programa de Investigación Pesquera, Universidad Austral de Chile, Puerto Montt, Chile*
[g] *Instituto de Acuicultura, Universidad Austral de Chile, Puerto Montt, Chile*
[h] *Programa de Investigación Pesquera, Instituto de Acuicultura, Universidad Austral de Chile, Puerto Montt, Chile*
[i] *Centro Oceanográfico de Vigo, Instituto Español de Oceanografía (IEO-CSIC), Subida a Radio Faro 50, 36390, Vigo, Spain*

ARTICLE INFO

Keywords:
Resting cysts
Saxitoxins
Yessotoxins
Redox potential
Harmful algal blooms
Seasonality

ABSTRACT

Harmful algal blooms (HABs) are recurrent in the NW Patagonia fjords system and their frequency has increased over the last few decades. Outbreaks of HAB species such as *Alexandrium catenella*, a causal agent of paralytic shellfish poisoning, and *Protoceratium reticulatum*, a yessotoxins producer, have raised considerable concern due to their adverse socioeconomic consequences. Monitoring programs have mainly focused on their planktonic stages, but since these species produce benthic resting cysts, the factors influencing cyst distributions are increasingly gaining recognition as potentially important to HAB recurrence in some regions. Still, a holistic understanding of the physico-chemical conditions influencing cyst distribution in this region is lacking, especially as it relates to seasonal changes in drivers of cyst distributions, as the characteristics that favor cyst preservation in the sediment may change through the seasons. In this study, we analyzed the physico–chemical properties of the sediment (temperature, pH, redox potential) and measured the bottom dissolved oxygen levels in a "hotspot" area of southern Chile, sampling during the spring and summer as well as the fall and winter, to determine the role these factors may play as modulators of dinoflagellate cyst distribution, and specifically for the cysts of *A. catenella* and *P. reticulatum*. A permutational analysis of variance (PERMANOVA) showed the significant effect of sediment redox conditions in explaining the differences in the cyst assemblages between spring-summer and fall-winter periods (seasonality). In a generalized linear model (GLM), sediment redox potential and pH were associated with the highest abundances of *A. catenella* resting cysts in the spring-summer, however it was sediment temperature that most explained the distribution of *A. catenella* in the fall-winter. For *P. reticulatum*, only spring-summer sediment redox potential and temperature explained the variation in cyst abundances. The implications of environmental (physico-chemical) seasonality for the resting cysts dynamics of both species are discussed.

☆ This paper has been recommended for acceptance by Sarah Harmon.

* Corresponding author. Centro i~mar, Universidad de Los Lagos, Casilla 557, Puerto Montt, Chile.
E-mail address: camilorodriguezvillegas@gmail.com (C. Rodríguez–Villegas).

https://doi.org/10.1016/j.envpol.2022.119901
Received 22 April 2022; Received in revised form 1 August 2022; Accepted 2 August 2022

1. Introduction

Marine and freshwater dinoflagellates are a prominent group of phytoplankton with broad-ranging differences in their morphology, lifestyle, reproduction, toxin production, and nutritional requirements (D'Silva et al., 2011; Figueroa et al., 2018). They include autotrophic, heterotrophic, and mixotrophic species, most of which proliferate in the water column as haploid motile cells (Brosnahan et al., 2010; Shin et al., 2011). However, under specific conditions, some species enter into benthic cyst stages in which water-column communities are transformed, resulting in well-preserved communities in the sediments (Head, 1996; Matthiessen et al., 2005). This versatile life-cycle implies that the same species can be present in different forms, at different times, and in different environments, which would explain the spatio-temporal discontinuity in the abundances of some species in the water column (Boero et al., 1996).

While these habitat shifts are part of a meroplanktonic strategy of some dinoflagellates that allows benthic-planktonic habitat coupling, they are usually ignored in local monitoring programs, which are mainly focused on planktonic communities (Cembella et al., 2010; Yarimizu et al., 2020). However, contemporary surveys of cyst assemblages in sediments have provided evidence of rarely observed planktonic species, including those with only a brief motile life cycle, species that are so far unidentified, and those with difficult to identify vegetative forms (Dale, 1983). Moreover, sediment surveys may allow the detection of species responsible for harmful algal blooms (HABs), thus providing an early warning of potential toxic bloom events and/or the identification of toxigenic species new to the area (Dale, 2001; Ellegaard et al., 1994; Figueroa et al., 2018; Joyce et al., 2005).

Both in coastal and in offshore waters, HAB outbreaks are characterized by their expanded biogeographic range (area), long duration (intensity), high toxicity (severity), the presence of a large number of toxic species (diversity), and, more recently, their increasing rate of occurrence (frequency). These worrisome trends have been attributed to intensified monitoring as well as the rapid expansion of the marine aquaculture industry and other marine resources, and in part, also been attributed to anthropogenically induced climate change which has different species-specific responses to its environmental variations (Anderson et al., 2012b; Berdalet et al., 2017; Figueroa et al., 2018; Glibert and Burford, 2017; Hallegraeff, 1993; Hallegraeff et al., 2021; Heisler et al., 2008; Kudela et al., 2015; Smayda, 1990; Wells et al., 2020). This global tendency implies elevated costs for HAB mitigation strategies and other management actions, given the threat posed by HABs to fisheries, ecosystems, and human health (Heisler et al., 2008; Trainer et al., 2020; Young et al., 2020). Nowadays, the need for both regional and species-level investigations remains (Hallegraeff et al., 2021).

The north-western Patagonian fjords system is also threatened by HABs (Díaz et al., 2019; FAO, 2020). High-density outbreaks of cyst-forming dinoflagellates, including toxic species such as *Alexandrium catenella* (Whedon & Kofoid) Balech 1985, a saxitoxin (STX) producer responsible for paralytic shellfish poisoning (PSP), and the yessotoxin (YTX) producers *Protoceratium reticulatum* (Claparède & Lachmann) Bütschli, 1885*, Lingulodinium polyedrum* (F. Stein) J.D. Dodge, 1989*, Gonyaulax taylorii* M.C. Carbonell-Moore, 1996*,* and *G. spinifera* (Claparède & Lachmann) Diesing, 1866 (Álvarez et al., 2016; Guzmán et al., 2002; Paz et al., 2008; Satake et al., 1997; Tubaro et al., 2010), have been reported in the region together with blooms of the non-toxic cosmopolitan genus *Scripsiella* spp., Balech ex A.R.Loeblich III, 1965, whose high abundances can lead to oxygen depletion in the water column (and therefore fish kills) (Hallegraeff, 1992). These events represent a significant and growing threat to the regional aquaculture industry, artisanal fisheries, and seafood production of north-west Patagonia and thus to human health.

In areas of frequent bloom episodes, the sediments are likely to be seedbeds for the respective species. High vegetative cell densities ($>1 \times 10^6$ cell L^{-1}) and encystment rates together lead to the accumulation of high abundances of cysts in the sediments (Genovesi-Giunti et al., 2006). After their endogenous dormancy requirements are fulfilled and when environmental conditions are appropriate, excystment (cyst germination) can serve as a planktonic inoculum that may give rise to a new bloom. Thus, recognition of the link between planktonic and benthic stages is a first step in HAB mitigation (Head, 1996; Varela et al., 2012).

However, the role of benthic cysts in explaining bloom recurrence is controversial. In some cases, dinoflagellate cysts were shown to be of little importance in bloom initiation (Hesse et al., 1997), including by *A. catenella* in the NW Patagonian fjords system. Laboratory experiments showed variations in the sexual compatibility of strains with high resting cyst production (max. ~ 98×10^3 resting cysts L^{-1}), while in field studies, after an intense bloom leading to high levels of PSP and high resting cyst production during the bloom decline phase (Rodríguez-Villegas et al., 2020; Rodríguez-Villegas et al., 2021a), there was no evidence of large cyst seedbeds in the sediments (Alves-de-Souza et al., 2008; Cembella et al., 2010; Díaz et al., 2014; Díaz et al., 2018; Seguel et al., 2015). The exception was the detection of a high concentration of *A. catenella* resting cysts in the sediments a year after an intense bloom in 2009, although cyst densities decreased rapidly (within 90 days) (Díaz et al., 2014; Mardones et al., 2016). Thus, at least for *A. catenella* in this area, resting cysts do not seem to substantially contribute to bloom recurrence, perhaps due to local physical and hydrological conditions that hinder cyst preservation (Díaz et al., 2018). Nonetheless, interactions between resting cysts and the biological and physico-chemical conditions of the sediments are often ignored in studies of HABs, but they must be considered to explain the spatio-temporal dynamics of bloom events (Persson, 2000).

If resting cyst abundance reflects cyst production (Díaz et al., 2014) and both are closely related to bloom intensity (Mardones et al., 2016), then the 2016 bloom of *A. catenella*—one of the most intense to be registered in the NW Patagonia fjord system (5×10^6 cells^{-1}) and one of the most toxic bloom events recorded (15×10^3 μg STX eq. 100 g^{-1}; Buschmann et al., 2016)—should have given rise to important cyst beds in the sediments of the bloom site. Thus, in the present study, using data obtained 7 months after the 2016 *A. catenella* bloom, we assessed the temporal variability (seasonality) in the abundance of dinoflagellate cyst assemblages and its relationship to the physico-chemical characteristics of the sediment, including granulometry, redox potential, temperature, and pH. In addition, given the potential for toxic HAB outbreaks of *A. catenella* and *P. reticulatum* in the NW Patagonian fjords system, we examined the co-occurrence of these species in the sediments in terms of cyst abundance and distribution.

2. Material and methods

2.1. Survey area

The south austral region encompasses ~241,000 km^2, of which ~100,200 km^2 are located in NW Patagonia (41.5–45.0°S) (Fig. 1). The latter includes one of the most extensive fjords and channels system on Earth (Pantoja et al., 2011; Silva and Vargas, 2014) and hosts a high level of primary production, especially during spring-summer (Aracena et al., 2011). Four water masses cover the salinity range well described by Pérez-Santos et al. (2014). Large-volume freshwater inputs derive from rainfall (1000–7000 mm yr^{-1} Aracena et al. (2011)), glacial melting, streamflow from the Puelo (678 $m^3\ s^{-1}$) and Petrohue (278 $m^3\ s^{-1}$) rivers toward Reloncaví Fjord in the north (41.4 °S), including from the Yelcho (363 $m^3\ s^{-1}$) and Palena (43.6 °S) rivers entering Corcovado gulf, and, at the southern end of NW Patagonia, from the Cisnes River flowing to Puyuhuapi Fjord (45.0 °S) (Pantoja et al., 2011) (Fig. 1).

Another relevant feature of NW Patagonia is the abrupt change in the complexity of the coastline, which includes archipelagos such as the Desertores Islands, located in the inner Chiloé Sea (50- to 60-km wide), and the Guatecas Islands, located at the north-west end of Moraleda

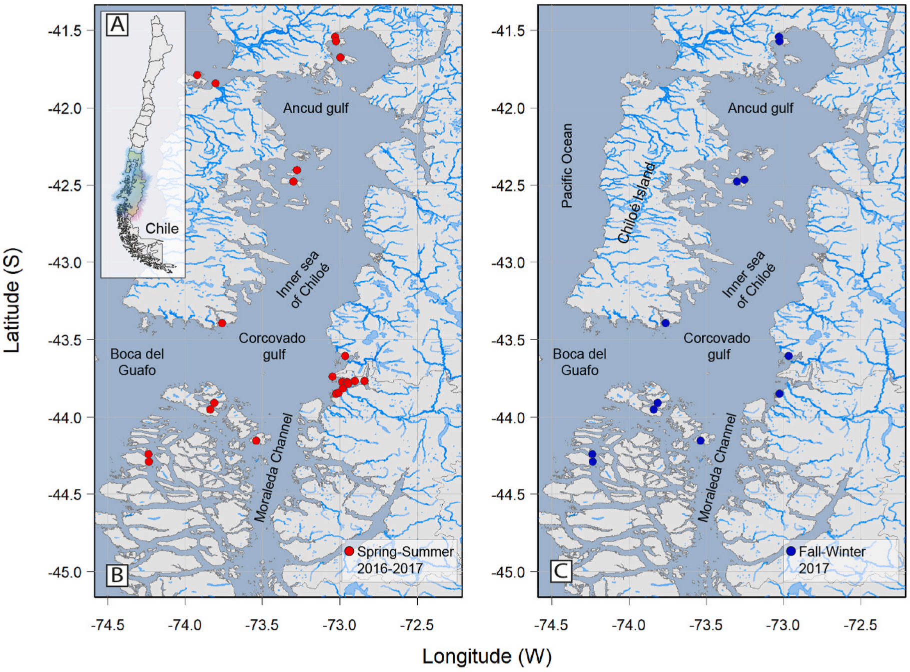

Fig. 1. Survey area in southern Chile. The shaded area within continental Chile shows the Los Lagos and Aysén regions (A). Maps of the sampling stations and the hydrography (lakes and rivers) of the sediment sampling sites in spring-summer 2016 (B) and fall-winter 2017 (C).

Channel (13- to 25-km wide) (Strub et al., 2019). The submarine topography of this area is also complex, as it is strongly influenced by oceanic waters flowing through Boca del Guafo and connecting both the Chiloé Sea in the north and Moraleda Channel in the south (Pickard, 1971; Rodrigo, 2006). The latter acts as a transition channel that mediates the transport and exchange of freshwater coming mainly from Puyuhuapi Fjord (Schneider et al., 2014).

In recent years, NW Patagonia has been claimed by an increasing number of stakeholders, mainly mussel and salmon farmers and the ecotourism industry. Dinoflagellate bloom events threaten not only these activities but also the ecosystems of NW Patagonia's fjords and channels. It is therefore essential that decision-makers develop conservation measures that are based on solid scientific knowledge (Iriarte et al., 2010; Pantoja et al., 2011).

2.2. Field sampling

Recent sediments were sampled at 37 stations from NW Patagonian fjords during two different oceanographic campaigns: in the austral spring–summer of 2016–2017 (SS) and in the fall–winter of 2017 (FW). At each sampling station ($n = 24$ for SS; and $n = 13$ for FW, Fig. 1B, C) sediment samples were collected from three different 0.1-m^2 sites using a Van Veen grab (SO-MET Company, Chile). The samples were used to determine dinoflagellate resting cysts, granulometry, total organic matter (TOM), sediment temperature, pH, and redox potential (redox). Simultaneously, two 250-mL water subsamples were taken 1 m from the bottom with a 10-L Go-flo oceanographic bottle and used to measure dissolved oxygen (DO) according to the Carpenter (1965) technique. All station depths were measured onboard with an Echo Sounder (Garmin® Striker Plus 4cv).

Sediment temperature, pH, and redox potential were measured in triplicate using a pre-calibrated portable multi-parameter MultiLine meter (Multi 3620 IDS probe, WTW) fitted with electrodes designed to analyze semisolids. A conical electrode fitted with Teflon, fiber, and ceramic triple-union conical electrodes was used to measure the pH; the temperature was recorded automatically by the instrument. Sediment redox was determined using a platinum sensor and Ag/AgCl saturated (3.5 M KCL) gel/polymer electrolyte. All measurements were made following the recommendations of the Chilean standard ISO NCh: 17025 of 2005 and those described by of Søndergaard (2009).

After the physico-chemical parameters had been determined, a dark plastic corer (8 cm length, 6 cm diameter) was used to obtain three undisturbed sub-samples from each grab to examine their content of dinoflagellate resting cysts (described below). To avoid stimulating germination of the resting cysts by oxygen, light, or temperature changes, each sub-sample was manually released of air bubbles, wrapped in aluminum foil, and preserved at 4 °C until analyzed (Anderson et al., 2003). These conditions were shown to be effective in maintaining cyst quiescence (Anderson et al., 1987). Granulometry and TOC were determined in 500 cm^{-3} of grab sediment as described below.

2.3. Sediment grain size and total organic content

Sediment samples were freeze-dried and then analyzed using a series of sieves (2000, 1000, 500, 250, 150, 90, and 63 μm). Each sample was shaken for 15 min in a mechanical sieve shaker (Gilson Company, Inc.). The weight of the sediment fraction retained in each sieve and in the pan (<63 μm) was then used to calculate the granulometry of that fraction using the "rysgran" R package (De Camargo, 2016).

The grain size composition of the sediment was categorized using the Wentworth (1922) system as follows: gravel $\geq$2000 μm; very coarse sand >1000 < 2000 μm; coarse sand >500 < 1000 μm; medium sand >250 < 500 μm; fine sand >125 < 250 μm; very fine sand >63 < 125 μm; and silt $\leq$63 μm. Based on these categories, grain size (phi, Φ) parameters were calculated according to the proportion of each sediment category as follows: $\Phi = -\log_2$ (grain size category in mm) × (proportion of each category, in %) (Krumbein, 1938). This method was shown to be suitable for statistical analyses and graphical representations of sediment samples containing a wide range of grain sizes, with higher or lower Φ values representing sediment samples with a predominantly finer or coarser grain size, respectively (Donoghue, 2016). To characterize the sediment at each sampling station, the results obtained for the three sediment subsamples were averaged and graphically represented for SS and FW.

TOM (%) was estimated based on the loss on ignition, determined following the recommendations of the RAMA (Accompanying

Resolution N°404 of Environmental Regulation for Aquaculture N°3411/2006). Briefly, sediment samples were air-dried at 60 °C for 72 h, weighed, and then heated in a muffle furnace at 450 °C for 6 h to burn the organic matter and obtain the ashes. The resultant ash weight was registered and the TOM (%) was calculated based on the difference between the dry weight and the weight of the calcined sample.

2.4. Sediment processing and dinoflagellate cyst counting

Dinoflagellate cysts were extracted from the first 3 cm of the sediment, corresponding to the layer susceptible to cyst resuspension and thus as the source of a new bloom (Anderson et al., 2014), following the procedures outlined by (Matsuoka and Fukuyo, 2000), with slight modifications. Thus, 3 cm^3 of sediment sample was suspended in 0.2 μM filtered seawater, sonicated (Labsonic 1000 L/Braun Sonic) for 1 min, and then washed through sieves of 106 μm and 20 μm mesh. Since most known cysts are 25–100 μM in length (Ellegaard et al., 1994), the content retained on the last sieve was transferred to a Petri dish. The cysts were kept in suspension in the filtered seawater by swirling the plates, which caused heavy sediment particles to remain at the center of the dish bottom, while the cysts remained suspended in the circulating water. The suspension was transferred to a 50-ml glass graduated cylinder, to which filtered seawater was then added to achieve a final volume of 20 ml. The cyst content of three 1-ml subsamples was analyzed using a Sedgewick-Rafter counting chamber and an inverted microscope with phase-contrast illumination (Olympus CKX41). Only dinoflagellate cysts with an intact cytoplasmic content were considered viable (Anderson et al., 1987; Genovesi-Giunti et al., 2006).

2.5. Data analysis

The effects of environmental parameters on the dinoflagellate cyst assemblages obtained during the SS vs. FW oceanographic campaigns were compared in a constrained analysis of proximities (CAP) in the Jaccard distance matrix using the “capscale” function in the “vegan” package from R (Anderson and Willis, 2003; Legendre and Anderson, 1999). The CAP is an exploratory ordination method, useful to visualize the effect of some variables (redox, pH, temperature, and sediment Φ) over the entire cysts community, without a hypothesis test.

The influence of physico-chemical variables (redox, pH, temperature, sediment Φ) on the species composition of dinoflagellate benthic cysts was assessed in a marginal permutational analysis of variance (PERMANOVA) based on Jaccard dissimilarities (Anderson, 2014; Paliy and Shankar, 2016), using the “adonis2” function from the R package “vegan” (Oksanen et al., 2018). An empirical pseudo-*F* distribution and *p*-values were calculated from 10,000 permutations (Oksanen et al., 2018). The robustness of PERMANOVA hypothesis test lies in the work with ecological/field data severely non-normal and zero-inflated (see Anderson, 2014), with the advantage of gaining statistical resolution because allows the identification of the contribution of specific variables over the cysts community.

A generalized linear model (GLM) with a log link function and negative binomial distribution (McCullagh and Nelder, 1989) was implemented to evaluate the influence of different environmental factors on the prevalence of *A. catenella* and *P. reticulatum* cysts in the study area. The explanatory variables were the same as those described above for the resting cyst community. Homoscedasticity was tested in a Levene’s test, and collinearity in a variance inflation test (VIF), using a threshold VIF ≤ 4 (Fox and Weisberg, 2011). Data overdispersion was assessed by comparing observed and expected dispersion values (Crawley, 2007; Venables and Ripley, 2010).

Only main effects were included in the model because interactions between many variables risked obscuring their effects (Gotelli and Ellison, 2004). The effects of the explanatory variables were tested using a marginal test -type II ANOVA- (Venables and Ripley, 2013).

Data on the physico-chemical properties of the sediment and the bottom dissolved oxygen content were graphically represented using Ocean Data View with a surface view and applying diva gridding interpolation (Schlitzer, 2019). Statistical analyses were conducted using the statistical and programming software R 2.1.12 (R Core Team, 2019), available through the CRAN repository (http://www.r-project.org). Following the recommendations of the American Statistical Association (Wasserstein and Lazar, 2016) and an increasing number of scientists worldwide (Amrhein et al., 2019), a dichotomic use of *p*-values was avoided; instead, the values are provided as calculated, except when several values were summarized within a single group.

Median values and the inter-quartile range (IQR) were used to report the physico-chemical properties of the sediment and the bottom dissolved oxygen content, and arithmetic means and standard deviations to report dinoflagellate cyst abundances.

3. Results

3.1. Sediment physico-chemical parameters and bottom dissolved oxygen content

The grain size composition in the study area was mostly mud and sand, with a low proportion of very coarse sand or gravel, for both SS and FW samples (Fig. 2A). The highest TOM value determined in SS samples was 1.63%, measured in the inner sea of Chiloé, and that in FW samples 1.86%, measured in Melinka, Guaitecas Archipelago (Fig. 2A). The median sediment Φ was 323.3 (IQR = 81.62) for the SS samples and 288.1 (IQR = 123.9) for the FW samples, indicating the finer grain size of a larger proportion of SS than FW sediments (Fig. 2B).

The median depth of the all sampling stations differed only by ~3 m between SS and FW, suggesting that the two sets of samples were comparable. The median depth of SS sampling was 42 m (IQR = 11.65 m) and that of FW sampling 45 m (IQR = 17 m) (Fig. 2C). The deepest sampling stations of the SS and FW campaign were located at Betecoi Island, in the Guaitecas Archipelago (Aysén region), with depths of 65 m and 66 m, respectively.

The median sediment temperature was 12.25 °C (IQR = 0.28 °C) during SS sampling and 11.9 °C (IQR = 0.30 °C) during FW sampling (Fig. 2D; Table S1). For both SS and FW, a meridional spatial pattern was identified that was characterized by a gradient of warmer sediments in the north (41.5°S) and cooler sediments in the south (44.3°S) (Fig. S1A, B). The main difference was an east-west zonal strip of warmer sediment of ~0.4° located between 43.6°S and 43.9°S (Fig. S1A). The highest sediment temperature for SS was 13.86 °C, measured at Lagreze Channel (Aysén region), while for FW it was 12.36 °C, measured at Tic Toc Bay (Los Lagos region) (Fig. 2D and, Fig. S1A, B).

The median pH of the sediment was 7.3 (IQR = 0.23) for SS and 7.35 (IQR = 0.19) for FW (Fig. 2E; Table S1). For both SS and FW samples, a zonal east-west spatial pattern was identified consisting of a gradient from less to more alkaline sediments (Fig. S1C, D). The SS and FW patterns differed in the amplitude of the gradient, which was wider for SS for FW sediments (Fig. S1c, d). The highest sediment pH among the SS samples was 7.78, measured at the Lagreze Channel (Aysén region) while for FW it was 7.62, measured at San Pedro (Los Lagos region) (Fig. 2E and, Fig. S1C, D).

The median sediment redox for SS samples was 220 mV (IQR = 221.6 mV) and that of FW samples 130 mV (IQR = 115 mv) (Fig. 2F; Table S1). In either case, the redox values did not follow an obvious zonal or meridional spatial pattern but oxic and anoxic areas could be identified during both sampling seasons (Fig. S1E, F). Oxic sediments were predominately located east of the Moraleda Channel (Aysén region) and northwards of the inner sea of Chiloé (Los Lagos region), and anoxic sediments around the Guaitecas Archipelago (Aysén region) (Fig. S1E, F). The highest sediment redox value for the SS samples was 427.2 mV, determined at the Ensenada sampling station (Aysén region), and that for the FW samples 370 mV, determined at San Pedro (Los Lagos region) (Fig. 2F, Fig. S1E, F).

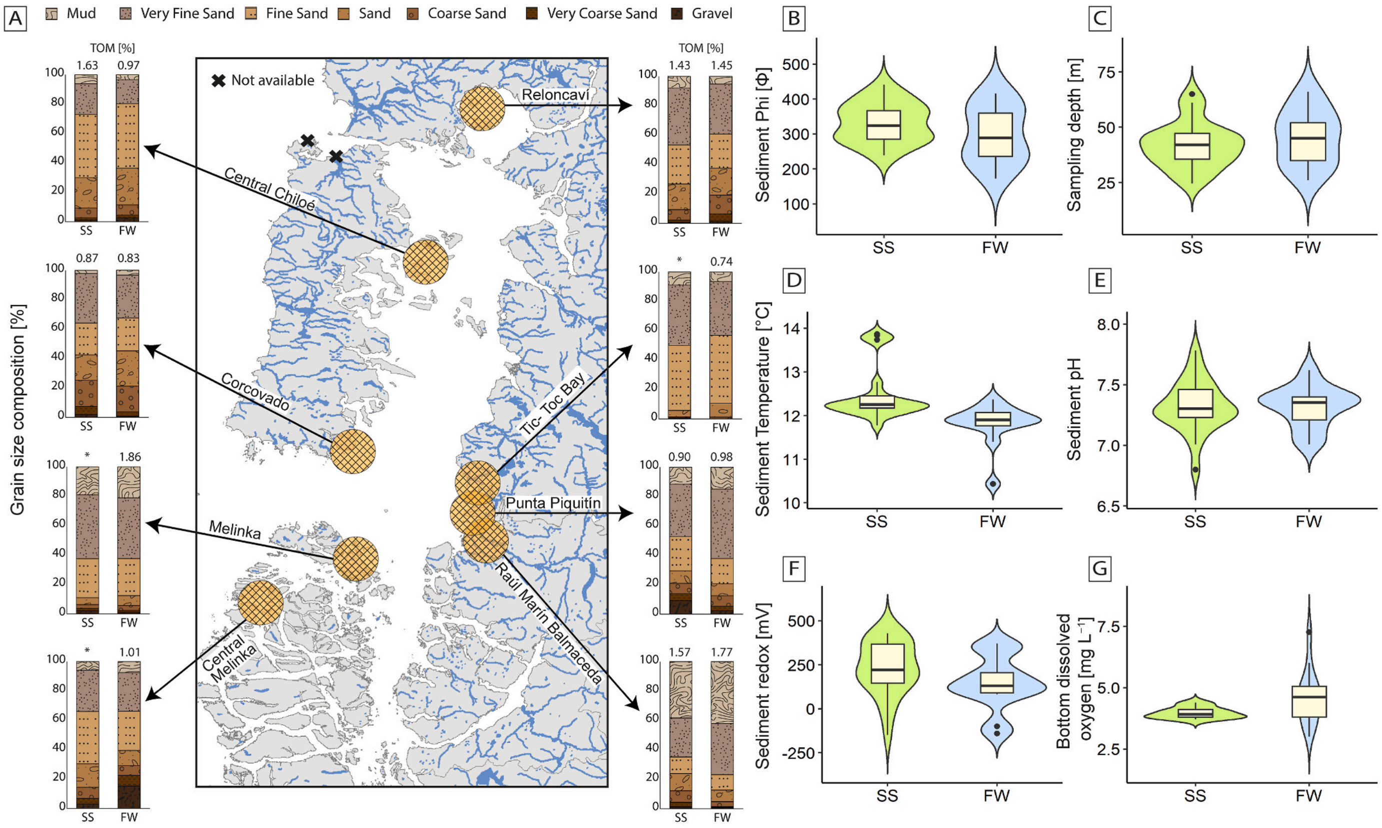

Fig. 2. Physico-chemical characteristics of sediments collected from the survey area in spring-summer (SS) and fall-winter (FW). (A) Grain size composition and total organic matter (TOM) [%] according to SS and FW sampling locations. An asterisk above the bars denotes not available data. Violin plots of sediment phi [Φ] (B); sampling station depth (C), sediment temperature [°C] (D), pH (E), redox potential [mV] (F), and the bottom dissolved oxygen level [mg/L] (G), showing the range (lines extending from the bars), median (bold lines), and interquartile range (box height) and outlining the probability density. Details of the specific geographic coordinates and number of sampling stations for each location and sampling season are provided in Fig. 1.

The median bottom DO content of the SS samples was 3.9 mg/L (IQR = 0.31 mg/L) and that of the FW samples 4.6 mg/L (IQR = 1.25 mg/L) (Fig. 2G). For the former, a meridional spatial pattern was identified, characterized by a higher DO in the north (41.5°S) than in the south (44.3°S). For FW, a zonal pattern was observed in which the DO concentrations increased from east to west, except at Guaitecas Archipelago, where the DO values were low, and at Raúl Marín Balmaceda sampling stations, where the DO values were higher (Fig. S1G, H). The highest DO among the SS samples was 4.38 mg/L, measured at the Meulin sampling station in the inner sea of Chiloé (Los Lagos region). Among the FW samples, DO was highest (7.26 mg/L) at May Island (Aysén region) (Fig. 2G, Fig. S1G, H).

3.2. *Dinoflagellate benthic cyst abundance and species richness*

In the analysis of dinoflagellate cysts in sediment samples from SS and FW, five orders belonging to 18 genera were detected: Gonyaucales, Gymnodiniales, Peridiniales, Pyrocystales, and Suessiales. Among the 50 different morphotypes, 34 were identified to the species level, 4 to the genus level and 12 remained unidentified (Table 1; Fig. 3–5). The dinoflagellate cyst assemblages were dominated by heterotrophic taxa (~28 species), of which *Protoperidinium* Bergh, 1881, was the most diverse genus, with 12 species and 3 morphotypes. The autotrophic genus *Scrippsiella* Balech ex Loeblich III, 1965, comprised 4 species and 1 morphotype, and the heterotrophs *Archaeperidinum* (Kofoid) Jorgensen 1912, and *Selenopemphix* P. N. Benedek, 1972, 2 species each (Table 1; Fig. 3, 4). The other recorded genera were *Alexandrium* Halim, 1960, *Protoceratium* Bergh, 1881*, Spiniferites* G. A. Mantell, 1850*, Gonyaulax* Diesing, 1866*, Lingulodinium* D. Wall, 1967*, Polykrikos* Buetschli, 1873*, Pentapharsodinium* Indelicato and Loeblich, III, 1986*, Brigantedinium* Matsuoka ex Head (1996)*, Preperidinium* Mangin, 1913*, Diplopsalopsis* Meunier, 1910*, Niea* Kawami, Iwataki et Matsuoka*,* and *Dissodinium* Klebs, 1916, (recorded for the first time in NW Patagonia) (Table 1).

Dinoflagellate cysts were detected at all sampling stations during the SS and FW surveys. Their total abundances ranged from 6 to 1852 (306.3 ± 475.0; $n = 24$) and from 18 to 2300 (546.0 ± 781.8; $n = 13$), respectively (Table 1). The highest cyst abundances, determined in both the SS and FW samples, were found at the northern end of the study area (~41.6°S), adjacent to Reloncaví Sound (Fig. 6A, B). The species cf. *L. polyedrum* (F.Stein) J.D.Dodge, 1989*, Scrippsiella lachrymosa* J. Lewis, 1991*, Scrippsiella precaria* M. Montresor & A. Zingone, 1988*,* and *Protoperidinium* sp. 2, and *Protoperidinium* sp. 7 were detected in the FW but not in the SS samples while the species *Protoperidinium punctulatum* (Paulsen, 1907) Balech, 1974*, Protoperidinium* sp. 6, *Brigantedinium asymmetricum* Matsuoka ex Head (1996)*, Selenopemphix undulata* T. J. Verleye, V. Pospelova, K. N. Mertens & S. Louwye, 2011*,* and *Selenopemphix tholus* Bradford, 1975, were detected in the SS but not in the FW samples (Table 1).

The CAP ordination showed marked differences in the species composition of dinoflagellate cysts collected during SS vs. FW (Fig. 7A, B). Cumulatively, the first two axes represented 81.3% and 35.0%, respectively, of the variation in the Jaccard distance matrix of dinoflagellate cysts (Fig. 7A, B). In the analysis of SS samples, two environments could be distinguished: one characterized by the correlation of Φ, temperature, and pH (top left), and the other by redox (bottom left) (Fig. 7A). The abundances of toxigenic species such as *A. catenella* and *P. reticulatum* increased as redox decreased. The analysis of FW samples revealed three environments and one gradient: the first environment

Table 1
Nutritional strategy (a: autotrophic; h: heterotrophic; m: mixotrophic) and mean abundance (cysts cm^{-3}) of 50 types of dinoflagellates resting cysts obtained during spring-summer (SS) and fall-winter (FW) oceanographic campaigns. The abundance of empty dinoflagellate resting cysts is shown in parentheses; (−): missing records.

Sampling station			Meulin		Guar		San Pedro		Maillen		I. Sanchez		Chincuí		Caguach		Betecoi	
	Nutrition	Code	SS	FW	SS	FW	SS	FW	SS	FW	SS	FW	SS	FW	SS	FW	SS	FW
Gonyaucales																		
Alexandrium catenella (Wedon & Kofoid) Balech	a	Acat	0	-	0	-	0	2	0	0	26(4)	15	0	0	3	0	0(3)	12(8)
Protoceratium reticulatum (Claparece & Lachmann) Bütschli	a	Pret	3 (6)	-	11 (574)	-	0 (6)	0 (8)	30 (264)	23 (284)	26 (740)	30 (455)	39 (305)	8 (402)	0 (6)	0 (2)	42 (261)	76 (480)
Spiniferites ramosus	a	Sram	0	-	112	-	0	0	12	23	0	0	88	54	0	0	0	4
Gonyaulax spinifera (Claparece & Lachmann)	a	Gspi	0	-	0	-	0	0	0	12	0	0	4	10	0	0	0	0
cf. *Lingulodinium polyedrum*	a	Lpol	0	-	0	-	0	0	0	0	0	5	0	0	0	0	0	0
Gymndiniales																		
Polykrikos schwartzii Bütschli	h	Psch	12	-	35	-	9	8	12	23	26	35	77	34	6	2	33	52
Polykrikos kofoidii	h	Pkof	0	-	0	-	0	0	0	0	0	0	0	4	0	0	0	0
Peridiniales																		
Pentapharsodinium dalei indelicato *et* Loeblich III	h	Pdal	3	-	60	-	3	6	18	69	0	5	98	72	3	2	18	8
Scrippsiella trochoidea (Stein) Loeblich III	a	Stro	0	-	0	-	0	0	0	19	0	0	4	10	0	0	0	0
*Scrippsiella patagonica*Akselman *et* Keupp	a	Spat	0	-	0	-	0	0	12	46	0	0	28	68	9	0	0	0
Scrippsiella lachrymosa J. Lewis ex Head	a	Slac	0	-	0	-	0	0	0	0	0	0	0	0	0	0	0	4
Scrippsiella precaria Montresor & Zingone	a	Spre	0	-	0	-	0	4	0	0	0	0	0	0	0	0	0	0
Scrippsiella spp.	a	Sspp	3	-	39	-	0	0	0	8	4	15	4	0	0	0	0	0
Brigantedinium asymmetricum Reid	h	Basy	3	-	0	-	0	0	0	0	0	0	0	0	0	0	0	0
Archaeperidinium minutum (Kofoid) Jørgensen	h	Amin	21	-	1344	-	3	8	372	1564	204	105	780	1689	15	24	90	140
Archaeperidinium constrictum (Abé)	h	Acon	0	-	4	-	0	0	12	0	0	0	7	0	0	0	0	12
Protoperidinium americanum (Gran & Baraaud) Balech	h	Pame	15	-	21	-	3	10	0	8	17	5	39	12	24	4	39	52
Protoperidinium avellana (Meunier) Balech	h	Pave	15	-	14	-	9	14	42	23	26	45	74	20	30	2	36	36
Protoperidinium claudicans (Paulsen) Balech	h	Pcla	6	-	11	-	0	0	0	0	9	5	11	10	0	0	0	0
Protoperidinium conicoides (Gran) Balech	h	Pcon	0	-	14	-	0	0	0	8	0	0	18	8	0	2	12	12
Protoperidinium conicum (Gran) Balech	h	Pcni	6	-	46	-	0	6	18	31	43	20	39	28	27	12	12	16
Protoperidinium denticulatum (Gran & Baraaud) Balech	h	Pden	6	-	7	-	3	2	0	0	9	0	25	0	6	0	15	8
Protoperidinium excentricum (Paulsen) Balech	h	Pexc	3	-	21	-	3	0	6	46	43	10	32	26	15	6	27	16
Protoperidinium leonis (Pavillard) Balech	h	Pleo	3	-	4	-	0	2	0	0	0	0	7	0	0	0	9	8
Protoperidinium oblongum	h	Pobl	0	-	0	-	0	0	0	0	9	0	0	0	0	0	0	0
Protoperidinium pentagonum (Gran) Balech	h	Ppen	3	-	7	-	0	0	0	31	9	10	18	16	6	2	9	16
Protoperidinium subinerme (Paulsen) Loeblich III	h	Psub	3	-	4	-	0	0	0	0	0	0	0	2	0	2	9	8
Protoperidinium punctulatum	h	Ppun	0	-	7	-	3	0	0	0	0	0	11	0	0	0	0	0
Protoperidinium spp.	h	Pspp	6	-	11	-	3	6	30	15	17	30	25	24	18	0	36	56
Protoperidinium sp. 2	h	Psp2	0	-	0	-	0	0	0	0	0	0	0	0	0	0	0	0
Protoperidinium sp. 6	h	Psp6	0	-	0	-	0	0	0	0	0	0	0	0	0	0	3	0
Protoperidinium sp.7	h	Psp7	0	-	0	-	0	0	0	0	0	0	0	0	0	0	0	0
Preperidinium meunieri	h	Pmeu	6	-	25	-	6	2	24	4	43	15	60	18	3	4	15	16
Diplopsalopsis ovata (Abé)	h	Dova	3	-	0	-	3	0	0	0	0	5	0	0	0	0	0	0
Niea acanthocysta (Kawami, Iwataki & Matsuoka)	h	Naca	0	-	0	-	0	0	0	4	9	0	0	2	0	0	3	4
Selenopemphix undulata	h	Sund	0	-	0	-	0	0	0	0	4	0	0	0	0	0	0	0
Selenopemphix tholus	h	Stho	0	-	0	-	0	0	0	0	4	0	0	0	0	0	0	0
Pyrocystales																		
Dissodinium pseudolunula Elbrächter & Drebes	h	Dpse	0	-	4	-	0	0	0	115	0	0	0	54	0	0	0	0
Unidentified cysts																		
Unidintified 1	-	Un01	0	-	4	-	0	0	6	15	0	5	11	2	0	0	3	0
Unidintified 2	-	Un02	3	-	25	-	0	0	0	15	162	85	14	0	15	0	42	16
Unidintified 9	-	Un09	0	-	0	-	3	0	0	0	0	0	0	0	0	0	0	0
Unidintified 10	-	Un10	0	-	0	-	0	0	0	15	4	0	4	0	0	0	0	0
Unidintified 13	-	Un13	3	-	0	-	0	2	6	15	0	5	7	0	6	2	0	12
Unidintified14	-	Un14	0	-	0	-	0	0	0	0	0	0	0	0	0	0	0	0
Unidintified 19	-	Un19	0	-	0	-	0	0	0	0	9	0	0	0	3	0	0	0

(*continued on next page*)

Table 1 (*continued*)

Sampling station			Meulin		Guar		San Pedro		Maillen		I. Sanchez		Chincuí		Caguach		Betecoi	
	Nutrition	Code	SS	FW	SS	FW	SS	FW	SS	FW	SS	FW	SS	FW	SS	FW	SS	FW
Unidintified 25	-	Un25	0	-	11	-	0	0	6	0	0	0	32	30	0	0	0	0
Unidintified 27	-	Un27	0	-	0	-	0	0	0	61	0	0	0	6	0	140	0	72
Unidintified 33	-	Un33	0	-	4	-	0	0	0	92	0	0	0	0	0	0	0	0
Unidintified 34	-	Un34	9	-	7	-	0	0	6	0	0	0	7	6	6	0	0	0
Unidintified 35	-	Un35	3	-	0	-	3	0	0	15	17	10	0	4	0	0	3	0

Sampling station			C. Colorado		P. Huala		Las Varas		Añihué 156		Añihué 153		Ensenada 19		Ensenada Bol.	
	Nutrition	Code	SS	FW	SS	FW	SS	FW	SS	FW	SS	FW	SS	FW	SS	FW
Gonyaucales																
Alexandrium catenella (Wedon & Kofoid) Balech	a	Acat	0	-	0	-	0	-	0	-	0	-	0	-	0	-
Protoceratium reticulatum (Claparece & Lachmann) Bütschli	a	Pret	0	-	0	-	0	-	0	-	0	-	0	-	0(32)	-
Spiniferites ramosus	a	Sram	0	-	0	-	0	-	0	-	0	-	0	-	0	-
Gonyaulax spinifera (Claparece & Lachmann)	a	Gspi	5	-	0	-	0	-	0	-	0	-	0	-	0	-
cf. *Lingulodinium polyedrum*	a	Lpol	0	-	0	-	0	-	0	-	0	-	0	-	0	-
Gymndiniales																
Polykrikos schwartzii Bütschli	h	Psch	0	-	4	-	0	-	0	-	0	-	0	-	0	-
Polykrikos kofoidii	h	Pkof	0	-	0	-	0	-	0	-	0	-	0	-	0	-
Peridiniales																
Pentapharsodinium dalei indelicato *et* Loeblich III	h	Pdal	0	-	4	-	0	-	0	-	0	-	0	-	0	-
Scrippsiella trochoidea (Stein) Loeblich III	a	Stro	0	-	0	-	0	-	0	-	0	-	5	-	0	-
*Scrippsiella patagonica*Akselman *et* Keupp	a	Spat	0	-	0	-	0	-	0	-	0	-	0	-	5	-
Scrippsiella lachrymosa J. Lewis ex Head	a	Slac	0	-	0	-	0	-	0	-	0	-	0	-	0	-
Scrippsiella precaria Montresor & Zingone	a	Spre	0	-	0	-	0	-	0	-	0	-	0	-	0	-
Scrippsiella spp.	a	Sspp	0	-	0	-	0	-	0	-	0	-	0	-	0	-
Brigantedinium asymmetricum Reid	h	Basy	0	-	0	-	0	-	0	-	0	-	0	-	0	-
Archaeperidinium minutum (Kofoid) Jørgensen	h	Amin	5	-	4	-	0	-	0	-	0	-	5	-	0	-
Archaeperidinium constrictum (Abé)	h	Acon	0	-	0	-	0	-	0	-	0	-	0	-	0	-
Protoperidinium americanum (Gran & Baraaud) Balech	h	Pame	0	-	12	-	0	-	5	-	9	-	23	-	0	-
Protoperidinium avellana (Meunier) Balech	h	Pave	15	-	12	-	0	-	5	-	9	-	45	-	5	-
Protoperidinium claudicans (Paulsen) Balech	h	Pcla	0	-	0	-	0	-	0	-	0	-	0	-	0	-
Protoperidinium conicoides (Gran) Balech	h	Pcon	0	-	4	-	0	-	0	-	0	-	0	-	5	-
Protoperidinium conicum (Gran) Balech	h	Pcni	0	-	4	-	0	-	0	-	0	-	5	-	0	-
Protoperidinium denticulatum (Gran & Baraaud) Balech	h	Pden	0	-	4	-	0	-	0	-	9	-	0	-	0	-
Protoperidinium excentricum (Paulsen) Balech	h	Pexc	0	-	0	-	3	-	0	-	0	-	9	-	27	-
Protoperidinium leonis (Pavillard) Balech	h	Pleo	0	-	0	-	0	-	0	-	0	-	0	-	0	-
Protoperidinium oblongum	h	Pobl	0	-	0	-	0	-	0	-	0	-	0	-	0	-
Protoperidinium pentagonum (Gran) Balech	h	Ppen	0	-	0	-	0	-	0	-	0	-	0	-	0	-
Protoperidinium subinerme (Paulsen) Loeblich III	h	Psub	0	-	0	-	0	-	0	-	0	-	5	-	0	-
Protoperidinium punctulatum	h	Ppun	0	-	0	-	0	-	0	-	9	-	0	-	0	-
Protoperidinium spp.	h	Pspp	5	-	20	-	0	-	0	-	27	-	9	-	0	-
Protoperidinium sp. 2	h	Psp2	0	-	0	-	0	-	0	-	0	-	0	-	0	-
Protoperidinium sp. 6	h	Psp6	0	-	0	-	0	-	0	-	0	-	0	-	0	-
Protoperidinium sp.7	h	Psp7	0	-	0	-	0	-	0	-	0	-	0	-	0	-
Preperidinium meunieri	h	Pmeu	0	-	4	-	0	-	0	-	9	-	14	-	5	-
Diplopsalopsis ovata (Abé)	h	Dova	0	-	0	-	0	-	0	-	18	-	0	-	0	-
Niea acanthocysta (Kawami, Iwataki & Matsuoka)	h	Naca	0	-	0	-	0	-	0	-	0	-	0	-	0	-
Selenopemphix undulata	h	Sund	0	-	0	-	0	-	0	-	0	-	0	-	0	-
Selenopemphix tholus	h	Stho	0	-	0	-	0	-	0	-	0	-	0	-	0	-
Pyrocystales																
Dissodinium pseudolunula Elbrächter & Drebes	h	Dpse	0	-	0	-	0	-	0	-	0	-	0	-	0	-
Unidentified cysts																
Unidintified 1	-	Un01	5	-	0	-	3	-	0	-	0	-	9	-	9	-
Unidintified 2	-	Un02	0	-	0	-	0	-	0	-	0	-	0	-	0	-

(*continued on next page*)

Table 1 (*continued*)

Sampling station			C. Colorado		P. Huala		Las Varas		Añihué 156		Añihué 153		Ensenada 19		Ensenada Bol.	
	Nutrition	Code	SS	FW	SS	FW	SS	FW	SS	FW	SS	FW	SS	FW	SS	FW
Unidintified 9	-	Un09	0	-	0	-	0	-	0	-	0	-	5	-	0	-
Unidintified 10	-	Un10	0	-	0	-	0	-	0	-	9	-	0	-	0	-
Unidintified 13	-	Un13	0	-	4	-	0	-	0	-	0	-	0	-	0	-
Unidintified14	-	Un14	0	-	4	-	0	-	0	-	0	-	0	-	5	-
Unidintified 19	-	Un19	0	-	0	-	0	-	0	-	0	-	0	-	0	-
Unidintified 25	-	Un25	0	-	0	-	0	-	0	-	0	-	0	-	0	-
Unidintified 27	-	Un27	0	-	4	-	0	-	0	-	0	-	0	-	0	-
Unidintified 33	-	Un33	0	-	0	-	0	-	0	-	0	-	0	-	5	-
Unidintified 34	-	Un34	0	-	0	-	9	-	0	-	0	-	5	-	0	-
Unidintified 35	-	Un35	0	-	0	-	0	-	0	-	0	-	0	-	0	-

Sampling station			Hermanas 112		Hermanas 34		Cochinos		Yuste		I. May		Lagrese		Forsyth		Tic Toc		RMB 3		RMB		Teuquelín	
	Nutrition	Code	SS	FW	SS	FW	SS	FW	SS	FW	SS	FW	SS	FW	SS	FW	SS	FW	SS	FW	SS	FW	SS	FW
Gonyaucales																								
Alexandrium catenella (Wedon & Kofoid) Balech	a	Acat	0	-	0	-	0	-	2 (44)	-	11	5(8)	15	0	9	33	0	2	0	-	-	0	-	0
Protoceratium reticulatum (Claparece & Lachmann) Bütschli	a	Pret	0	-	0 (6)	-	0	-	0	-	0 (144)	0 (53)	9 (138)	2 (52)	0 (106)	18 (123)	0 (2)	0 (2)	0	-	-	0 (4)	-	0
Spiniferites ramosus	a	Sram	0	-	0	-	0	-	0	-	0	3	0	0	0	0	0	0	0	-	-	0	-	2
Gonyaulax spinifera (Claparece & Lachmann)	a	Gspi	0	-	0	-	0	-	0	-	0	0	0	0	0	0	0	0	0	-	-	0	-	0
cf. *Lingulodinium polyedrum*	a	Lpol	0	–	0	-	0	-	0	-	0	0	0	0	0	0	0	0	0	-	-	0	-	0
Gymndiniales																								
Polykrikos schwartzii Bütschli	h	Psch	0	-	0	-	0	-	0	-	25	8	3	2	21	8	14	8	24	-	-	38	-	0
Polykrikos kofoidii	h	Pkof	0	-	0	-	0	-	0	-	0	0	3	0	0	0	0	0	0	-	-	0	-	0
Peridiniales																								
Pentapharsodinium dalei indelicato *et* Loeblich III	h	Pdal	0	-	6	-	0	-	2	-	7	0	21	7	0	8	11	8	24	-	-	21	-	0
Scrippsiella trochoidea (Stein) Loeblich III	a	Stro	0	-	0	-	0	-	0	-	0	0	3	0	0	0	4	0	0	-	-	0	-	0
*Scrippsiella patagonica*Akselman *et* Keupp	a	Spat	0	-	0	-	0	-	0	-	0	0	0	2	0	0	0	0	0	-	-	0	-	0
Scrippsiella lachrymosa J. Lewis ex Head	a	Slac	0	-	0	-	0	-	0	-	0	0	0	0	0	0	0	2	0	-	-	0	-	0
Scrippsiella precaria Montresor & Zingone	a	Spre	0	-	0	-	0	-	0	-	0	0	0	0	0	0	0	0	0	-	-	0	-	2
Scrippsiella spp.	a	Sspp	0	-	0	-	0	-	0	-	0	0	0	0	0	0	0	0	0	-	-	9	-	0
Brigantedinium asymmetricum Reid	h	Basy	0	-	0	-	0	-	0	-	0	0	3	0	0	0	0	0	0	-	-	0	-	0
Archaeperidinium minutum (Kofoid) Jørgensen	h	Amin	0	-	12	-	4	-	3	-	32	8	42	20	30	15	25	12	32	-	-	64	-	4
Archaeperidinium constrictum (Abé)	h	Acon	0	-	0	-	0	-	0	-	0	0	3	0	0	0	0	0	0	-	-	0	-	0
Protoperidinium americanum (Gran & Baraaud) Balech	h	Pame	0	-	6	-	0	-	0	-	0	0	12	0	9	13	32	6	40	-	-	38	-	0
Protoperidinium avellana (Meunier) Balech	h	Pave	0	-	6	-	0	-	0	-	11	8	12	4	13	3	11	12	112	-	-	85	-	2
Protoperidinium claudicans (Paulsen) Balech	h	Pcla	0	-	0	-	0	-	2	-	0	0	0	0	0	0	4	0	0	-	-	0	-	0
Protoperidinium conicoides (Gran) Balech	h	Pcon	0	-	12	-	1	-	0	-	7	0	12	7	4	0	0	0	32	-	-	0	-	2
Protoperidinium conicum (Gran) Balech	h	Pcni	0	-	0	-	1	-	2	-	7	0	12	2	0	40	7	0	8	-	-	9	-	0
Protoperidinium denticulatum (Gran & Baraaud) Balech	h	Pden	0	-	0	-	0	-	0	-	0	3	3	2	9	3	0	0	64	-	-	17	-	0
	h	Pexc	0	-	0	-	0	-	2	-	14	5	15	4	17	10	4	4	0	-	-	4	-	0

(*continued on next page*)

Table 1 (*continued*)

Sampling station			Hermanas 112		Hermanas 34		Cochinos		Yuste		I. May		Lagrese		Forsyth		Tic Toc		RMB 3		RMB		Teuquelín	
	Nutrition	Code	SS	FW	SS	FW	SS	FW	SS	FW	SS	FW	SS	FW	SS	FW	SS	FW	SS	FW	SS	FW	SS	FW
Protoperidinium excentricum (Paulsen) Balech																								
Protoperidinium leonis (Pavillard) Balech	h	Pleo	0	-	0	-	0	-	0	-	0	3	3	2	0	0	0	0	16	-	-	0	-	0
Protoperidinium oblongum	h	Pobl	0	-	0	-	0	-	0	-	0	0	3	0	0	0	0	0	0	-	-	0	-	2
Protoperidinium pentagonum (Gran) Balech	h	Ppen	0	-	0	-	0	-	0	-	0	0	3	0	0	5	0	0	8	-	-	0	-	0
Protoperidinium subinerme (Paulsen) Loeblich III	h	Psub	0	-	0	-	0	-	2	-	7	0	0	0	0	0	0	0	0	-	-	0	-	0
Protoperidinium punctulatum	h	Ppun	0	-	0	-	0	-	0	-	0	0	6	0	0	0	4	0	0	-	-	0	-	0
Protoperidinium spp.	h	Pspp	6	-	0	-	1	-	2	-	11	13	36	4	13	23	14	6	64	-	-	64	-	2
Protoperidinium sp. 2	h	Psp2	0	-	0	-	0	-	0	-	0	0	0	0	0	8	0	0	0	-	-	0	-	0
Protoperidinium sp. 6	h	Psp6	0	-	0	-	0	-	0	-	0	0	0	0	0	0	0	0	0	-	-	0	-	0
Protoperidinium sp.7	h	Psp7	0	-	0	-	0	-	0	-	0	0	0	0	0	0	0	0	0	-	-	9	-	0
Preperidinium meunieri	h	Pmeu	0	-	0	-	0	-	3	-	25	13	18	2	0	10	0	0	8	-	-	0	-	0
Diplopsalopsis ovata (Abé)	h	Dova	0	-	0	-	0	-	2	-	0	0	3	0	0	0	4	0	0	-	-	0	-	0
Niea acanthocysta (Kawami, Iwataki & Matsuoka)	h	Naca	0	-	0	-	0	-	0	-	0	0	0	0	0	0	0	0	8	-	-	0	-	0
Selenopemphix undulata	h	Sund	0	-	0	-	0	-	0	-	0	0	0	0	0	0	0	0	0	-	-	0	-	0
Selenopemphix tholus	h	Stho	0	-	0	-	0	-	0	-	0	0	0	0	0	0	0	0	0	-	-	0	-	0
Pyrocystales																								
Dissodinium pseudolunula Elbrächter & Drebes	h	Dpse	0	-	0	-	0	-	0	-	0	0	0	0	0	0	0	0	0	-	-	0	-	0
Unidentified cysts																								
Unidintified 1	-	Un01	0	-	0	-	0	-	0	-	0	0	3	2	0	5	0	0	0	-	-	4	-	0
Unidintified 2	-	Un02	0	-	0	-	0	-	2	-	84	0	60	15	43	0	4	26	16	-	-	4	-	0
Unidintified 9	-	Un09	0	-	0	-	0	-	0	-	0	0	3	0	0	0	0	0	0	-	-	13	-	0
Unidintified 10	-	Un10	0	-	0	-	3	-	0	-	0	0	0	0	0	5	0	0	0	-	-	0	-	0
Unidintified 13	-	Un13	0	-	0	-	0	-	0	-	0	0	0	2	0	5	0	2	16	-	-	4	-	0
Unidintified14	-	Un14	0	-	6	-	0	-	0	-	4	0	0	0	0	0	4	0	8	-	-	13	-	0
Unidintified 19	-	Un19	0	-	0	-	0	-	0	-	18	8	0	0	0	0	0	0	0	-	-	0	-	0
Unidintified 25	-	Un25	0	-	0	-	0	-	0	-	0	0	0	0	0	0	0	0	0	-	-	0	-	0
Unidintified 27	-	Un27	0	-	0	-	0	-	0	-	0	0	0	15	0	0	0	0	0	-	-	0	-	2
Unidintified 33	-	Un33	0	-	0	-	0	-	0	-	0	0	0	0	0	0	0	0	0	-	-	0	-	0
Unidintified 34	-	Un34	0	-	0	-	1	-	0	-	0	0	0	0	4	0	0	0	8	-	-	4	-	0
Unidintified 35	-	Un35	0	-	0	-	0	-	0	-	0	0	35	0	0	0	0	0	8	-	-	0	-	0

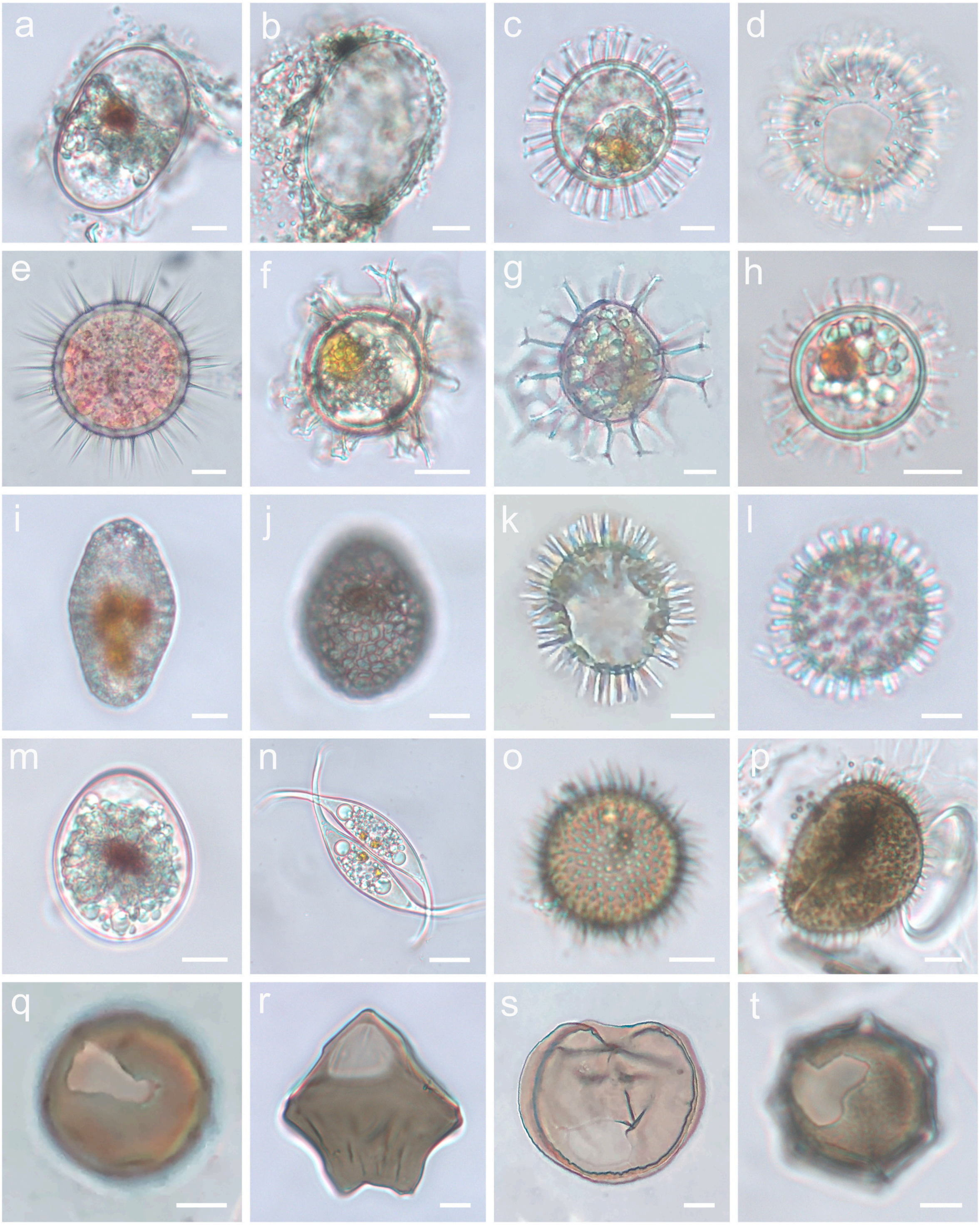

Fig. 3. (a) *Alexandrium catenella*. (b) *A. catenella* empty cyst. (c) *Protoceratium reticulatum*. (d) *P. reticulatum* empty cyst. (e) *Lingulodinium polyedrum*. (f) *Spiniferites pachydermus*. (g) *Spiniferites ramosus*. (h) *Pentapharsodinium dalei*. (i) *Scrippsiella lachrymosa*. (j) *Scrippsiella patagonica*. (k) *Scrippsiella precaria* empty cyst. (l) *Scrippsiella acuminata*. (m) *Scrippsiella* sp. (n) *Dissodinium pseudolunula*. (o) *Archaeperidinium minutum*. (p) *Archaeperidinium constrictum*. (q) *Brigantedinium symmetricum* empty cyst. (r) *Selenopemphix tholus* empty cyst. (s) *Selenopemphix undulata* empty cyst. (t) *Protoperidinium americanum* empty cyst. Scale bars: 10 μm, except (f) and (n): 20 μm.

was defined by the correlation of Φ and temperature (top left), the second by sediment pH (bottom left), and the third by redox (bottom right). The environmental gradient consisted of an inverse correlation between Φ and temperature with redox, implying that Φ and temperature values increased as the sediment redox decreased (Fig. 7A). Finally, the ordination plots showed that all dinoflagellate cyst species are not related to higher redox conditions or more oxygenated environments in both SS and FW samples.

According to the results of the PERMANOVA, redox ($p = 0.003$) had a strong influence on the species composition of dinoflagellate cyst communities in SS samples (Table 2), but there was no evidence of large effects for any predictor variable in FW samples (Table 2).

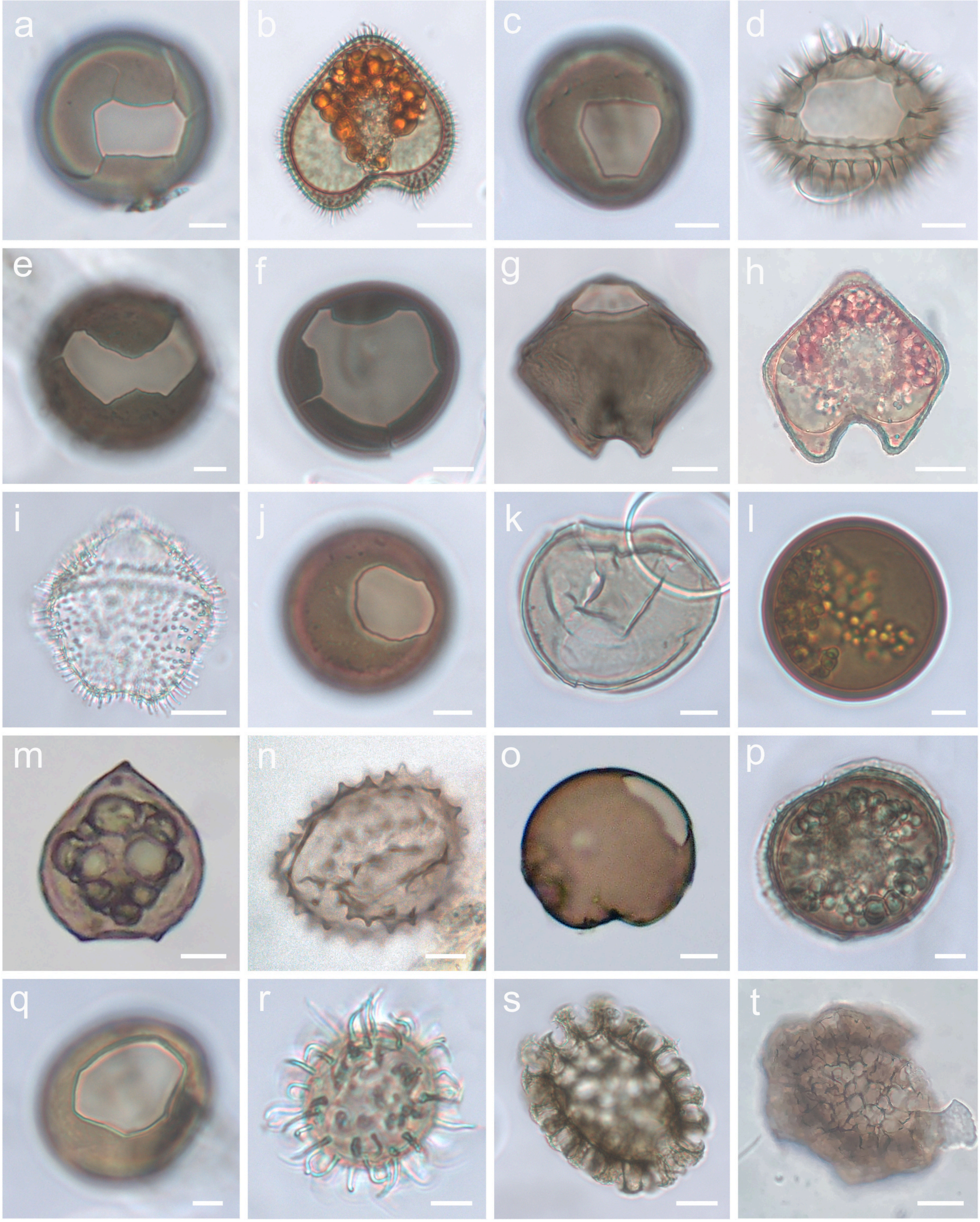

Fig. 4. (a) *Protoperidinium avellana* empty cyst. (b) *Protoperidinium claudicans*. (c) *Protoperidinium conicoides* empty cyst. (d) *Protoperidinium conicum* empty cyst. (e) *Protoperidinium denticulatum* empty cyst. (f) *Protoperidinium excentricum* empty cyst. (g) *Protoperidinium leonis* empty cyst. (h) *Protoperidinium oblongum* empty cyst. (i) *Protoperidinium pentagonum* empty cyst. (j) *Protoperidinium punctulatum* empty cyst. (k) *Protoperidinium subinerme*. (l) Round brown cyst. (m) *Protoperidinium* sp. X. (n) *Protoperidinium* sp. XX. (o) *Protoperidinium* sp. XXX. (p) *Preperidinium meunieri*. (q) *Diplopsalopsis ovata*. (r) *Niea acanthocysta*. (s) *Polykrikos schwartzii*. (t) *Polykrikos kofoidii*. Scale bars: 10 μm, except (b), (d), (g–i), (s) and (t): 20 μm. (For interpretation of the references to color in this figure legend, the reader is referred to the Web version of this article.)

3.3. *Toxigenic species*

Among the HAB species, *A. catenella* resting cysts were found during both SS and FW, with abundances ranging from 2 to 26 resting cysts cm^{-3} (2.86 ± 6.37; $n = 24$) and 2–33 resting cysts cm^{-3} (5.30 ± 9.68; $n = 13$), respectively (Fig. 6C, D). Empty resting cysts of *A. catenella* were detected as well (Fig. 3B), with a total abundance of 51 resting cysts cm^{-3} during SS and 16 resting cysts cm^{-3} during FW (Fig. 8A, B). From the 51 empty cysts recorded in SS samples, 44 were from Yuste Bay, the northwestern-most sampling station in the Los Lagos region (Fig. 8A).

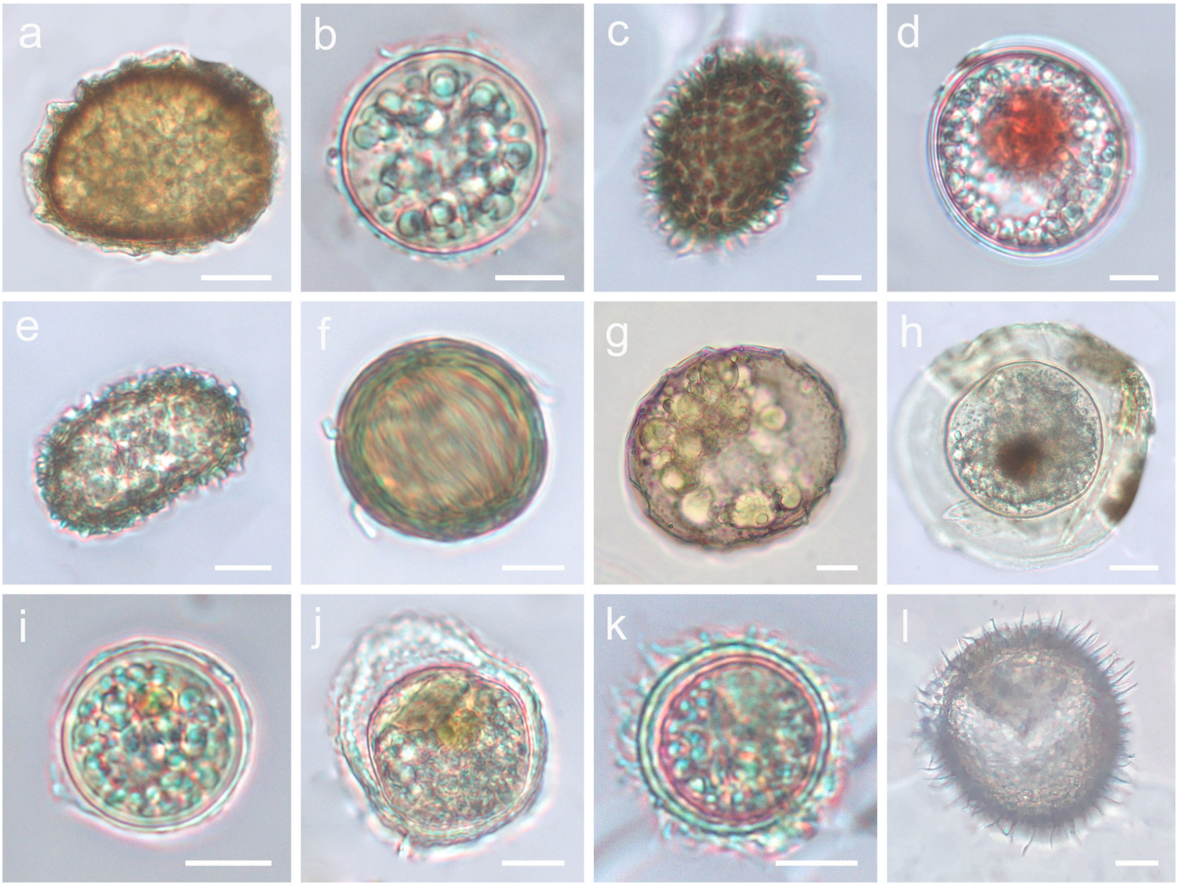

Fig. 5. (a) Unidentified cyst 1. (b) Unidentified cyst 2. (c) Unidentified cyst 9. (d) Unidentified cyst 14. (e) Unidentified cyst 19. (f) Unidentified cyst 25. (g) Unidentified cyst 27. (h) Unidentified cyst 33. (i) Unidentified cyst 34. (j) *Gymnodinium aureolum*. (k) *Biecheleria* spp. (l) Unidentified cyst 35. Scale bars: 10 μm, except (h) and (l): 20 μm.

From the 16 empty cysts in the FW samples, 8 were found at May Island, the southwestern-most sampling station in the Aysén region (Fig. 8B).

The abundances of HAB-forming *P. reticulatum* resting cysts during SS and FW were 3–42 (6.95 ± 13.19; $n = 24$) cysts cm^{-3} and 2–76 (12.23 ± 21.71; $n = 13$) cysts cm^{-3}, respectively (Fig. 8C, D). The highest abundance of empty cysts was 2590 cysts cm^{-3} and 1943 cysts cm^{-3}, respectively (Fig. 8C, D). From the empty cysts found during SS, 740 cysts cm^{-3} were present in samples from Sanchez Island, Guaitecas Archipelago (Aysén region) and 574 cysts cm^{-3} in those from Guar Island, adjacent to Reloncaví Sound (Los Lagos region) (Fig. 8C). Of the empty cysts obtained during FW, 480 cysts cm^{-3} were from Betecoi and 455 cysts cm^{-3} from Sanchez Island, both located in the Guaitecas Archipelago (Aysén region (Fig. 8D).

In the GLM models of HAB species, sediment redox ($p = 0.037$) and pH ($p = 0.051$) explained a significant fraction of the spatial variability observed in the *A. catenella* distribution during SS, and sediment temperature ($p = 0.044$) a significant fraction of that during FW (Table 3). None of the other predictor variables included in the models of either sampling season were significant. In the GLM models of the distribution of *P. reticulatum*, sediment redox ($p < 0.001$) and temperature ($p = 0.010$) were significant during SS but none of the predictor variables were significant during FW (Table 3).

4. Discussion

Dinoflagellate cysts exhibit a wide variety of phenotypes (e.g., in terms of shape, color, and ornamentation), physiology (e.g., toxin production), and resistance traits (e.g., storage products and resistant cell walls) that allow their adaptation to different environmental conditions and their survival and persistence in changing environments (Lundholm et al., 2011; Matsuoka and Fukuyo, 2000; Matsuoka and Fukuyo, 2003). Once the cyst dormancy period is fulfilled and environmental conditions are favorable, resting cysts may germinate and potentially become the inoculum of a new bloom event (Anderson et al., 2012a; Bravo and Figueroa, 2014). Considering that most of the 12 species responsible for the recent global and regional expansions of HAB events in the oceans (Smayda, 1997) are also present in the NW Patagonian fjords system, studies of their dynamics are crucial in efforts to mitigate the risk of HABs. However, the physico-chemical and biological interactions involved in the ecology of cyst-forming dinoflagellates at the sediment level are mostly unknown (Persson, 2000; Rodríguez-Villegas et al., 2021b). Therefore, in this study we analyzed the physico-chemical characteristics of the sediments (redox, temperature, and pH) in NW Patagonia during all four seasons and established their relationship to the abundances of heterotrophic, autotrophic, and toxigenic dinoflagellate species. Our aim was to determine if the physico-chemical sediment conditions driving the spatial patterns of resting cyst deposits vary by seasonally.

Our seasonal survey of the distribution of resting cyst assemblages in the NW Patagonian fjords system revealed the importance of the redox potential, particularly during SS (Table 2). In marine sediments, oxygen availability decreases with increasing depth, such that redox follows a vertical gradient, with positive values at the top and a negative trend in deeper layers, regardless of the season (Diaz and Rosenberg, 1995). The redox values determined in this study are consistent with the seasonal trends of eutrophic lakes, in which the mean redox of the sediment surface (0–3 cm depth) was shown to be higher in summer (~250 mV) than in winter (Søndergaard, 2009). In an early analysis of the sediment

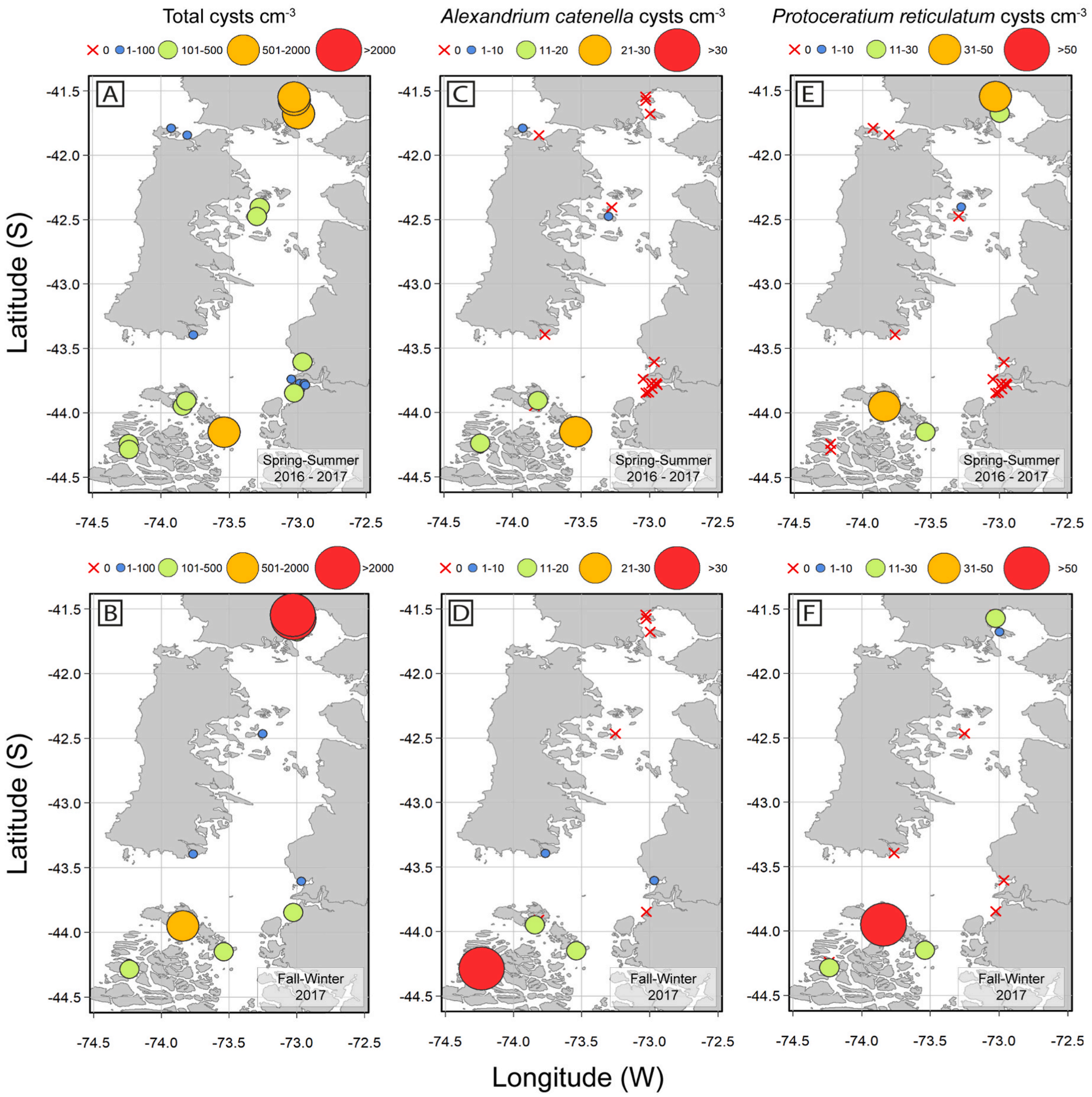

Fig. 6. Spatial variability in dinoflagellates cyst assemblages in the study area during spring-summer 2016 and fall-winter 2017. Total dinoflagellates cysts abundance (A, B). Cyst abundance of *A. catenella* (C, D). Cyst abundance of *P. reticulatum* (E, F). Note that the abundance scales differ for each plot.

of the NW Patagonian fjords system, ZoBell (1946) found positive redox values in oxygenated sediment deposits mostly characterized by a coarser grain size (lower Φ) and low organic matter content, and negative redox values in sediment deposits characterized by a fine grain size (higher Φ) and high organic matter content. These anoxic conditions often provide ideal conditions for hosting dinoflagellate cyst deposits (Persson, 2000; Rodríguez-Villegas et al., 2021b).

However, due to the dominance of *Archaeperidinium minutum* cysts at the sampling stations, total cyst abundances for SS and FW (500–2000 cysts cm^{-3}, Fig. 6A, B) were highest under oxygenated conditions (Fig. S1E). This finding agrees with those based on recent oceanographic expeditions, in which the abundance of *A. minutum* cysts was highest in fjord environments, where growth conditions, including enhanced rainfall and freshwater inputs, were optimal (Rodríguez-Villegas et al., 2021b, and references therein). To that end, *A. minutum* cysts were highly dominant at Guar, Maillen, and Chincuí, where 1344, 1564, and 1689 cysts cm^{-3}, respectively, were registered (see Table 1).

Nonetheless, total cyst abundance in anoxic sediments were also relatively high, both in SS and FW (100–500 cysts cm^{-3}; Fig. 6A, B, and Fig. S1E). Sediment oxygen levels are a critical determinant of cyst longevity (viability), degradation, and germination success (Anderson et al., 2003; Anderson et al., 1987; Gray et al., 2017; Keafer et al., 1992), and sediments from anoxic areas have been shown to generally favor the long-term survival of benthic cysts of many dinoflagellates species (Ellegaard et al., 2013). However, longevity is also a species-specific trait, involving factors such as the expression of small heat-shock proteins, which participate in cyst homeostasis during the dormancy period (Deng et al., 2021a, b), the robustness of the cell wall, and the amount of reserve material available for anaerobic respiration (starch grains, lipids). Environmental conditions also determine longevity, including predator presence or bioturbation activity (Dale, 2001; Head, 1996; Lundholm et al., 2011; Rodríguez-Villegas et al., 2021b), as discussed below, light and nutrient availability, temperature, and salinity [reviewed by Bravo and Figueroa (2014) and by Ellegaard and Ribeiro (2018)].

Even when most of the known cysts are 25–100 μm in length (the focus of the present study), many cysts species are smaller or even much smaller than 25 μm, such as *Biecheleria cincta, Biecheleriopsis adriatica,*

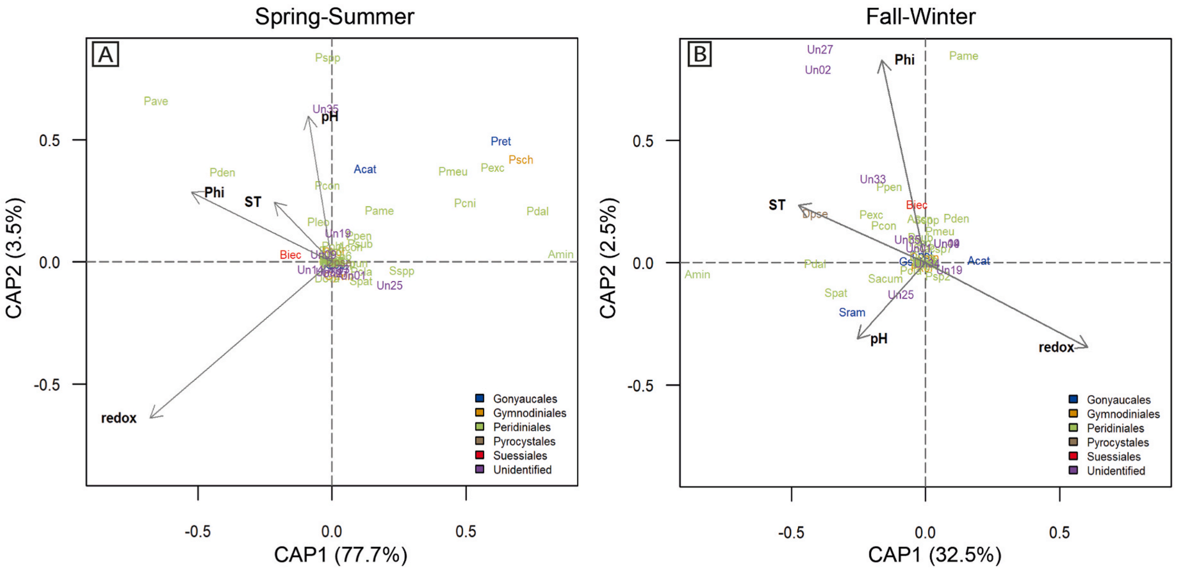

Fig. 7. Ordination biplot diagram of a constrained analysis of principal coordinates (CAP) in the Jaccard distance matrix, evaluating the effect of environmental variables on dinoflagellate benthic cyst assemblages determined in samples from oceanographic campaigns conducted in summer-spring (A) and fall-winter (B). ST: Sediment temperature. A key to the species names is provided in Table 1.

Table 2

PERMANOVA based on the Jaccard dissimilarities of the physico-chemical properties of the sediment harboring the resting cysts community (50 types), using 10,000 permutations for the hypothesis test.

Predictive variables	DF	Sum of squares	R^2	Pseudo - F	$Pr > F$
Spring-Summer					
Redox	1	0.695	0.081	1.912	0.003
Sediment temperature	1	0.360	0.042	0.991	0.471
Sediment pH	1	0.449	0.052	1.235	0.163
Phi	1	0.352	0.041	0.970	0.489
Residuals	18	6.545	0.770		
Total	22	8.492	1.000		
Fall-Winter					
Redox	1	0.302	0.067	0.798	0.730
Sediment temperature	1	0.344	0.077	0.907	0.579
Sediment pH	1	0.320	0.071	0.844	0.658
Phi	1	0.377	0.084	0.994	0.447
Residuals	8	3.033	0.679		
Total	12	4.465	1.000		

Cryptoperidiniopsis brodyi, Gyrodiniellum shiwhaense, Heterocapsa minima, Heterocapsa rotundata, Karenia mikimotoi, Karlodinium veneficum, Pelagodinium beii, Polarella glacialis, and *Gymnodinium simplex* (Liu et al., 2020a, b; Shang et al., 2019). This suggests that our methodological approach could underestimate or fail in detecting some species as described before that could be present in NW Patagonian fjords. Thus further studies need to consider a hybrid approach using light microscopy and molecular tools to avoid any bias in the abundance and the reported species.

Additionally, we are aware that other here unexplored drivers may be also relevant explaining the observed differences in resting cyst assemblages. For example, the accumulation of *Alexandrium* resting cysts seems to be favored by high organic matter content – a factor tightly related to oxygen levels (see for example Genovesi et al., 2013) - and high levels of pollutants (Zmerly et al., 2017), which are mainly transported to the sea sediments during the rainy season. Even if these factors have not been explicitly included here, and therefore, a specific study should be conducted to fully clarify their effect, the most novel result of the present work, which is a seasonal variation in the main factors affecting dinoflagellate resting cyst distribution, includes them indirectly. A detailed discussion about this effect ecological implications follows below.

4.1. Food-web implications of high abundances of heterotrophic species

Heterotrophic species of dinoflagellates are active grazers of vegetative stages of dinoflagellates (Gaines, 1987) including those of the toxigenic species *L. polyedrum* (Jeong et al., 1998) and *Gymnodinium catenatum* (Sampayo, 1998). Since heterotrophic species accounted for most of the dinoflagellate cysts (3:1 vs. autotrophic species), the presence of a high abundance of prey can be assumed. This was demonstrated in previous studies, in which a higher abundance of *Protoperidinium* spp. cysts in the sediments (as in this study) was consistent with a higher prey abundance, such as diatoms, in the water column (Alves-de-Souza et al., 2008; Krock et al., 2015).

These predator-prey interaction merit further studies, considering early observations of *Protoperidinium* spp. and the presence of different toxins (Dale, 2001). Although *P. crassipes* was initially identified as a producer of azaspiracid (AZA) (Ignatiades and Gotsis-Skretas, 2010), which causes azaspiracid shellfish poisoning (Hambright et al., 2014), it was later shown AZA was not produced endogenously by *P. crassipes* but instead originated from its phytoplankton prey (Gribble et al., 2007), the dinoflagellate *Azadinium* spp. (Tillmann et al. (2009). Similarly, detection of the toxins causing diarrheic shellfish poisoning in the heterotrophic dinoflagellates *P. oceanicum* and *P. pellucidum* may reflect their feeding on *Dinophysis* spp. (Van Egmond et al., 2004). These interactions must be elucidated in order to understand the ecological and biogeographical implications of cyst-forming dinoflagellates and their interactions with the surrounding environment, as changes in community composition can influence higher trophic levels (Dale, 1983; Klais et al., 2011; Kremp, 2013) and thus, directly or indirectly, aquaculture activities in the NW Patagonia fjords system.

4.2. Determinants of the co-occurrence of toxigenic species

The presence of toxigenic species such as *A. catenella* and *P. reticulatum* was explained by different physico-chemical drivers that can vary depending on the species, but also, and remarkably, by season. In the SS sampling period, for example, redox explained the abundances of both species in the NW Patagonian fjords system, yet only *A. catenella*

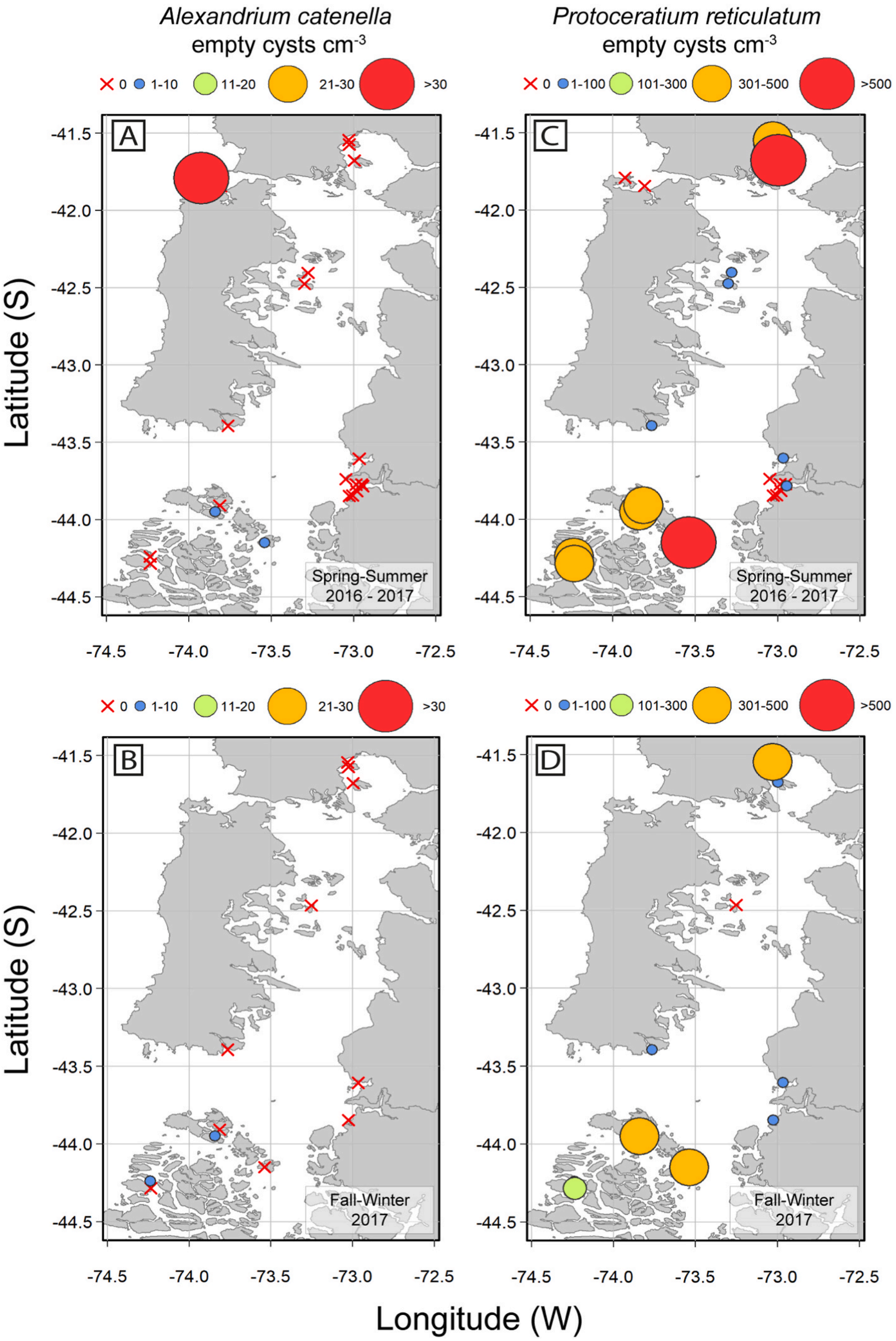

Fig. 8. Spatial variability of empty cysts of harmful species in the study area during spring-summer 2016 and fall-winter 2017. Abundance of empty cysts of *A. catenella* (A, B). Abundance of empty cysts of *P. reticulatum* (C, D). Note that the abundance scales differ for each plot.

was influenced by sediment pH and only *P. reticulatum* by sediment temperature (Table 3). During FW, however, it was sediment temperature that explained the abundance of *A. catenella*. Given this species-specific, and seasonally-specific complexity, these drivers were addressed individually below with emphasis on the seasonal variation of the factors driving toxigenic species abundance.

4.2.1. The seedbed hypothesis: implications for the recurrence of A. catenella blooms

Seven months after the largest bloom of *A. catenella* in the NW Patagonian fjords system thus far, there was no evidence of large seedbeds or empty cysts. This is in contrast to elsewhere in the world, where seedbeds, while spatially scattered, are a relatively constant presence in the sediments (Anderson et al., 2014). Although the residence time of *A. catenella* cysts in the sediments may depend on regional factors, our findings are nonetheless puzzling, given the intense outbreaks of STX-producing HABs recently recorded in the NW Patagonian fjords system. The intensity of these events drew international attention. For example, cell abundances in the 2016 bloom event reached 5×10^6 cells L^{-1} (see Buschmann et al., 2016), high enough to result in areas of cyst accumulation in the sediments. Indeed, this bloom was five orders of magnitude higher than that required for cyst accumulation zones in the sediments ($\sim 1 \times 10^6$ cell L^{-1}), as determined by Genovesi-Giunti et al. (2006). However, the abundances of resting cysts of *A. catenella* at the most northwestern sampling station (Yuste) and in the middle of the Desertores Islands corresponded only to minor remnants of the intense

Table 3
Statistical significance of explanatory variables determined using a X^2 test of a marginal (type II) ANOVA of the variability of the cyst abundances of the harmful species *Alexandrium catenella* and *Protoceratium reticulatum* in the sediment, using a generalized linear model (GLM) with a log link function for the residual negative binomial distribution.

Spring-Summer	***Alexandrium catenella***			***Protoceratium reticulatum***		
Predictive variables	Chi square X^2	DF	$Pr > (\|X^2\|)$	Chi square X^2	DF	$Pr > (\|X^2\|)$
Redox	4.309	1	0.037	143.3	1	<0.001
Sediment temperature	2.697	1	0.100	6.609	1	0.010
Sediment pH	3.801	1	0.051	0.140	1	0.708
Phi (Φ)	0.930	1	0.334	0.107	1	0.743
Fall-Winter						
Redox	1.096	1	0.295	2.324	1	0.127
Sediment temperature	4.043	1	0.044	1.135	1	0.286
Sediment pH	1.500	1	0.152	0.015	1	0.901
Phi (Φ)	2.043	1	0.220	0.1637	1	0.685

bloom of 2016 (Fig. 6A, B).

The low cyst abundances detected during SS and FW (max. ~33 cysts cm^{-3}) are consistent with other cyst surveys conducted in the area. Díaz et al. (2018) recorded only 8 cysts cm^{-3} in two different coastal systems (Guaitecas Archipelago and Pitipalena Fjord) of the Chilean inland sea after the bloom episode of December 2006–January-2007. Similarly, low abundances (51–128 cysts cm^{-3}) were found in exposed and protected localities (Low Bay and Ovalada Island) after the intense bloom event recorded of March–April 2009 that occurred in the Aysén region (Díaz et al., 2014). The highest abundance yet (68 cysts cm^{-3}) was recently determined in sediment samples from oceanic and fjord areas of NW Patagonia (Rodríguez-Villegas et al., 2021b). In their sediment surveys not linked to bloom occurrence, Cembella et al. (2010) found generally low resting cyst abundances (max. ~77 cysts cm^{-3}). Together, these results suggest that the dynamics of *A. catenella* resting cysts are mainly driven by local hydrodynamics (Genovesi et al., 2013), the relatively short maturation time of the resting cysts (69 days) (Mardones et al., 2016), and the predominantly high germination rates (Díaz et al., 2014).

Resting cysts in deeper layers of the sediments are typically older and may differ from the younger cysts buried in sediments closer to the surface. For example, in Sequim Bay, Washington, buried resting cysts of *Alexandrium* spp. (~41–50 cm depth, 28–42 years old), had a higher excystment success than cysts located in the surface sediment layers (~1–10 cm depth, < 1-year-old): ~42% vs. ~17% (Feifel et al., 2015). In Funka Bay, Hokkaido, Japan, Miyazono et al. (2012) found higher densities of morphologically unharmed *A. tamarense* cysts at a sediment depth of 22 cm (~50 years old). Following strong resuspension events, these cysts could act as a seed population able to fuel new bloom episodes.

The abundance of *A. catenella* resting cysts during SS was highest (26 cysts cm^{-3}) at Sanchez Island (Fig. 6C) and was associated with a positive redox (130 mV) and a lower pH (~7.2) of the sediments, conditions that likely favored the preservation of resting cysts (Persson, 2000). The scarcity of empty cysts at the same sampling station (~4 cysts cm^{-3}) (Table 1, Fig. 8A) may be related to the mandatory duration of dormant/quiescent periods, thus preventing cyst germination. However, the second highest abundance of *A. catenella* resting cysts (15 cysts cm^{-3}), at Lagreze (Fig. 6C), was found in sediments with negative redox conditions (−10 mV) and no empty cysts were detected (Fig. 8A). This suggests that environments with low oxygen levels accumulate resting cysts, which after resuspension events may germinate if the environmental conditions are appropriate and the dormancy period has been completed. A similar pattern in NW Patagonia was recently described for resting cysts of *A. catenella*, with higher abundances found in anoxic sediments, and lower abundances in oxygenated areas (Rodríguez-Villegas et al., 2021b).

In terms of temperature, the highest abundance of resting cysts (33 cysts cm^{-3}), recorded at the Forsyth sampling station (Fig. 6D) during FW, occurred in sediments with a relatively low temperature (~11.4 °C). Temperature is a key regulator of germination, and suboptimal temperatures may promote cyst quiescence, resulting in the permanence of cysts in the sediments (Kremp and Anderson, 2000). This was observed for cysts of the STX producer *Pyrodinium* spp., which occurred at high densities in sediments where temperatures were unfavorable for germination (Azanza et al., 2004).

4.2.2. Main drivers of *P. reticulatum* cyst abundances

The abundances of *P. reticulatum* cysts recorded in this study agreed with those obtained by Seguel et al. (2005), who recorded 5–90 cysts cm^{-3} at 6 of 20 sampling stations (~30%). Resting cysts of this species have also been observed in the waters of Argentina, including in the San Jorge Gulf (4 × 10^3 cysts g^{-1}; (Krock et al., 2015), and in the southwestern Atlantic (mean abundance: 94 cysts cm^{-3}; (Akselman et al., 2015). In our study, while cysts of *P. reticulatum* were detected in the inshore waters of NW Patagonia, their distribution in the sediments was very heterogeneous.

These results indicated that the highest abundance of *P. reticulatum* (42 cysts cm^{-3}, Betecoi) (Fig. 6E), detected during SS, was related to the negative redox (−150 mV) of one of the coolest sediments sampled during the SS campaign (~12.03 °C). The large presence of empty cysts at the same sampling station (261 cysts cm^{-3}) suggests that sediment conditions did not prevent germination. Rather, together with completion of the mandatory dormancy period, anoxia and the lower temperatures facilitated the maturation of *P. reticulatum* cysts. The mandatory dormancy of *P. reticulatum* as determined for Chilean strains under laboratory conditions is 123 ± 11 days (Salgado et al., 2017), such that it may have been completed before the detections of vegetative cells in the water column, both during warmer years, such as those corresponding to the El Niño Southern Oscillation (ENSO), and during the warmer season, i.e., austral summer (Alves-de-Souza et al., 2019; Alves-de-Souza et al., 2014). Indeed, recent surveys at the Atlantic Iberian Margin identified an association of *P. reticulatum* cysts with the warm stratified conditions of the water column (García-Moreiras et al., 2021). Moreover, the high abundance of *P. reticulatum* empty cysts can also be explained by their fossilizable properties, which would preserve them in the sediments (Head, 1996), resulting in the gradual accumulation of different cohorts over time (Ribeiro et al., 2013).

Finally, the observed seasonal variation in toxigenic cyst species could be explained by differences in the abundance of vegetative cells in the water column, in cyst production (mating/sexuality rates), and in encystment and therefore species-specific cyst sedimentation rates (Brosnahan et al., 2010; Joyce et al., 2005).

5. Conclusions

There was no evidence for the existence of a large-scale *A. catenella* seedbed after the intense bloom of 2016 in the NW Patagonia fjords system. However, each bloom episode is unique regarding its capability for resting cyst production and sedimentary storage, and thus, should be studied in depth. In this sense, the seasonality of the main factors affecting resting cyst abundances of toxigenic species is revealed by the present work as a novel result that should be taken into account in monitoring programs designed to provide early warnings of the potential for new bloom episodes. The high abundances of heterotrophic species recorded in this study are also a cause for concern, as the appearance of these species might precede that of toxigenic ones, posing a risk for higher trophic levels. Finally, subsurface accumulation of *A. catenella* resting cysts in NW Patagonia sediments also implies biological interactions with meiofauna, macrofauna, and bacterial communities, which merit further study.

Credit author statement

Camilo Rodríguez-Villegas: Conceptualization, Methodology, Software, Validation, Formal analysis, Investigation, Writing – original draft, Writing – review & editing, Visualization. **Patricio A. Díaz:** Conceptualization, Methodology, Software, Validation, Formal analysis, Investigation, Resources, Writing – original draft, Writing – review & editing, Visualization, Supervision. **Pablo Salgado:** Methodology, Software, Validation, Formal analysis, Investigation, Writing – original draft, Writing – review & editing. **Stephen J. Tomasetti:** Formal analysis, Investigation, Writing – original draft, Writing – review & editing. **Manuel Díaz:** Software, Formal analysis, Investigation, Visualization. **Sandra L. Marín:** Software, Formal analysis, Investigation, Visualization. **Ángela M. Baldrich:** Methodology, Software, Formal analysis, Investigation, Visualization. **Edwin Niklitschek:** Formal analysis, Investigation, Writing –original draft, Writing – review & editing. **Loreto Pino:** Software, Formal analysis, Investigation, Visualization. **Thamara Matamala:** Software, Formal analysis, Investigation, Visualization. **Katherine Espinosa:** Software, Formal analysis, Investigation, Visualization. **Rosa I. Figueroa**: Conceptualization, Methodology, Software, Validation, Formal analysis, Investigation, Resources, Writing – original draft, Writing – review & editing, Visualization.

Declaration of competing interest

The authors declare that they have no known competing financial interests or personal relationships that could have appeared to influence the work reported in this paper.

Data availability

Data will be made available on request.

Acknowledgments

This work was funded by the Fisheries Undersecretary of Chile by Fondo Investigación Pesquera y Acuicultura project [FIPA N°2016-02-ID 4728 _53_ LQ16] and by the Centro de Biotecnología y Bioingeniería (CeBiB) (PIA project FB0001, ANID, Chile). Rosa I. Figueroa was funded by a national project from the Spanish Ministry of Science and Innovation and the European Community (FEDER) (Project DIANAS-CTM2017-86066-R) and a grant for Galician Networks of Excellence (GRC-VGO-HAB IN607A-2019/04) from the Innovation Agency of the Xunta de Galicia (GAIN). The authors also acknowledge the Universidad Austral de Chile for the human and technical support of the oceanographic campaign. Camilo Rodríguez-Villegas had a fellowship from Universidad de Los Lagos.

Appendix A. Supplementary data

Supplementary data to this article can be found online at https://doi.org/10.1016/j.envpol.2022.119901.

References

Akselman, R., Krock, B., Alpermann, T.J., Tillmann, U., Borel, C.M., Almandoz, G.O., Ferrario, M.E., 2015. *Protoceratium reticulatum* (Dinophyceae) in the austral Southwestern Atlantic and the first report on YTX-production in shelf waters of Argentina. Harmful Algae 45, 40–52.

Álvarez, G., Uribe, E., Regueiro, J., Blanco, J., Fraga, S., 2016. *Gonyaulax taylorii*, a new yessotoxins-producer dinoflagellate species from Chilean waters. Harmful Algae 58, 8–15.

Alves-de-Souza, C., Iriarte, J.L., Mardones, J.I., 2019. Interannual variability of *Dinophysis acuminata* and *Protoceratium reticulatum* in a Chilean Fjord: insights from the realized niche analysis. Toxins 11, 19.

Alves-de-Souza, C., Varela, D., Contreras, C., de La Iglesia, P., Fernandez, P., Hipp, B., Hernandez, C., Riobó, P., Reguera, B., Franco, J.M., 2014. Seasonal variability of *Dinophysis* spp. and *Protoceratium reticulatum* associated to lipophilic shellfish toxins in a strongly stratified Chilean fjord. Deep Sea Res. Part II Top. Stud. Oceanogr. 101, 152–162.

Alves-de-Souza, C., Varela, D., Navarrete, F., Fernandez, P., Leal, P., 2008. Distribution, abundance and diversity of modern dinoflagellate cyst assemblages from southern Chile (43–54° S). Bot. Mar. 51, 399–410.

Amrhein, V., Greenland, S., McShane, B., 2019. Scientists rise up against statistical significance. Nature 567, 305–307.

Anderson, D., Fukuyo, Y., Matsuoka, K., 2003. Cyst methodologies. In: Manual on harmful marine microalgae, Monographs on oceanographic methodology, 11, 165-190.

Anderson, D.M., Alpermann, T.J., Cembella, A.D., Collos, Y., Masseret, E., Montresor, M., 2012a. The globally distributed genus *Alexandrium*: multifaceted roles in marine ecosystems and impacts on human health. Harmful Algae 14, 10–35.

Anderson, D.M., Cembella, A.D., Hallegraeff, G.M., 2012b. Progress in understanding harmful algal blooms: paradigm shifts and new technologies for research, monitoring, and management. Ann. Rev. Mar. Sci 4, 143–176.

Anderson, D.M., Keafer, B.A., Kleindinst, J.L., McGillicuddy Jr., D.J., Martin, J.L., Norton, K., Pilskaln, C.H., Smith, J.L., Sherwood, C.R., Butman, B., 2014. *Alexandrium fundyense* cysts in the Gulf of Maine: long-term time series of abundance and distribution, and linkages to past and future blooms. Deep Sea Res. Part II Top. Stud. Oceanogr. 103, 6–26.

Anderson, D.M., Taylor, C.D., Armbrust, E.V., 1987. The effects of darkness and anaerobiosis on dinoflagellate cyst germination. Limnol. Oceanogr. 32, 340–351.

Anderson, M.J., 2014. Permutational Multivariate Analysis of Variance (PERMANOVA). Wiley statsref: statistics reference online, pp. 1–15.

Anderson, M.J., Willis, T.J., 2003. Canonical analysis of principal coordinates: a useful method of constrained ordination for ecology. Ecology 84, 511–525.

Aracena, C., Lange, C.B., Iriarte, J.L., Rebolledo, L., Pantoja, S., 2011. Latitudinal patterns of export production recorded in surface sediments of the Chilean Patagonian fjords (41–55 S) as a response to water column productivity. Continent. Shelf Res. 31, 340–355.

Azanza, R.V., Siringan, F.P., Diego-Mcglone, M.L.S., Yñiguez, A.T., Macalalad, N.H., Zamora, P.B., Agustin, M.B., Matsuoka, K., 2004. Horizontal dinoflagellate cyst distribution, sediment characteristics and benthic flux in Manila Bay, Philippines. Phycol. Res. 52, 376–386.

Berdalet, E., Banas, N., Bresnan, E., Burford, M.A., Davidson, K., Gobler, C.J., Karlson, B., Kudela, R., Lim, P., Montresor, M., 2017. GlobalHAB, 2017. In: Berdalet et al (Ed.), Global Harmful Algal Blooms, Science and Implementation Plan. SCOR and IOC, Delaware and Paris, pp. 1–64.

Boero, F., Belmonte, G., Fanelli, G., Piraino, S., Rubino, F., 1996. The continuity of living matter and the discontinuities of its constituents: do plankton and benthos really exist? Trends Ecol. Evol. 11, 177–180.

Bravo, I., Figueroa, R., 2014. Towards an ecological understanding of dinoflagellate cyst functions. Microorganisms 2, 11–32.

Brosnahan, M.L., Kulis, D.M., Solow, A.R., Erdner, D.L., Percy, L., Lewis, J., Anderson, D.M., 2010. Outbreeding lethality between toxic Group I and nontoxic Group III *Alexandrium tamarense* spp. isolates: predominance of heterotypic encystment and implications for mating interactions and biogeography. Deep Sea Res. Part II Top. Stud. Oceanogr. 57, 175–189.

Buschmann, A., Farias, L., Tapia, F., Varela, D., Vasquez, M., 2016. Scientific report on the 2016 southern Chile red tide. Chil. Dep. Econ. 1–66. Available online: http://www.academiadeciencias.cl/wp-content/uploads/2017/04/InfoFinal_ComisionMareaRoja_21Nov2016.pdf.

Carpenter, J.H., 1965. The Chesapeake Bay Institute technique for the Winkler dissolved oxygen method. Limnol. Oceanogr. 10, 141–143.

Cembella, A., Guzmán, L., Roy, S., Diogène, J., 2010. GEOHAB Core Research Project: HABs in Fjords and Coastal Embayments.

Crawley, M., 2007. The R Book John Wiley & Sons, Chichester, UK.

D'Silva, M.S., Anil, A.C., D'Costa, P.M., 2011. An Overview of Dinoflagellate Cysts in Recent Sediments along the West Coast of India.

Dale, B., 1983. Dinoflagellate resting cysts:" benthic plankton. In: Survival Strategies of the Algae, pp. 69–136.

Dale, B., 2001. The sedimentary record of dinoflagellate cysts: looking back into the future of phytoplankton blooms. Sci. Mar. 65, 257–272.

De Camargo, M.G., 2016. SysGran: um sistema de código aberto para análises granulométricas do sedimento. Rev. Bras. Geociencias 36, 371–378.

Deng, Y., Li, F., Hu, Z., Yue, C., Tang, Y.Z., 2021a. Expression patterns of the heat shock protein 90 (Hsp90) gene suggest its possible involvement in maintaining the dormancy of dinoflagellate resting cysts. Int. J. Mol. Sci. 22, 11054.

Deng, Y., Li, F., Hu, Z., Yue, C., Tang, Y.Z., 2021b. The implication inferred from the expression of small heat-shock protein genes in dinoflagellate resting cysts buried in marine sediment. Diversity 13, 471.

Díaz, P., Molinet, C., Seguel, M., Dıaz, M., Labra, G., Figueroa, R.I., 2014. Coupling planktonic and benthic shifts during a bloom of *Alexandrium catenella* in southern Chile: implications for bloom dynamic and recurrence. Harmful Algae 40, 9–22.

Díaz, P.A., Álvarez, A., Varela, D., Pérez-Santos, I., Díaz, M., Molinet, C., Seguel, M., Aguilera-Belmonte, A., Guzmán, L., Uribe, E., 2019. Impacts of harmful algal blooms on the aquaculture industry: Chile as a case study. Perspect. Phycol. 6 (1–2), 39–50.

Díaz, P.A., Molinet, C., Seguel, M., Díaz, M., Labra, G., Figueroa, R.I., 2018. Species diversity and abundance of dinoflagellate resting cysts seven months after a bloom of *Alexandrium catenella* in two contrasting coastal systems of the Chilean Inland Sea. Eur. J. Phycol. 53, 410–421.

Diaz, R.J., Rosenberg, R., 1995. Marine benthic hypoxia: a review of its ecological effects and the behavioural responses of benthic macrofauna. Oceanogr. Mar. Biol. Annu. Rev. 33, 245-203.

Donoghue, J.F., 2016. Phi scale. In: Kennish, M.J. (Ed.), Encyclopedia of Estuaries. Springer Netherlands, Dordrecht, pp. 483–484.

Ellegaard, M., Christensen, N.F., Moestrup, Ø., 1994. Dinoflagellate cysts from Recent Danish marine sediments. Eur. J. Phycol. 29, 183–194.

Ellegaard, M., Ribeiro, S., 2018. The long-term persistence of phytoplankton resting stages in aquatic 'seed banks. Biol. Rev. 93, 166-183.

Ellegaard, M., Ribeiro, S., Lundholm, N., Andersen, T.J., Berge, T., Ekelund, F., Godhe, A., 2013. Using the sediment archive of living dinoflagellate cysts and other protist resting stages to study temporal population dynamics. Biol. Geol. perspect. dinoflagellates 149–153.

FAO, 2020. World Aquaculture Performance Indicators (WAPI) factsheet on aquaculture growth potential in Chile, pp. 1–76 online at. http://www.fao.org/73/ca8813en/ca8813en.pdf.

Feifel, K., Fletcher, S., Watson, L., Moore, S., Lessard, E., 2015. *Alexandrium* and *Scrippsiella* cyst viability and cytoplasmic fullness in a 60-cm sediment core from Sequim Bay, WA. Harmful Algae 47, 56–65.

Figueroa, R.I., Estrada, M., Garcés, E., 2018. Life histories of microalgal species causing harmful blooms: haploids, diploids and the relevance of benthic stages. Harmful Algae 73, 44–57.

Fox, J., Weisberg, S., 2011. An R Companion to Applied Regression. Sage, Thousand Oaks.

Gaines, G., 1987. Heterotrophic Nutrition. The Biology of Dinoflagellates.

García-Moreiras, I., Oliveira, A., Santos, A.I., Oliveira, P.B., Amorim, A., 2021. Environmental Factors Affecting Spatial Dinoflagellate Cyst Distribution in Surface Sediments Off Aveiro-Figueira da Foz (Atlantic Iberian Margin). Front. Mar. Sci. 1017.

Genovesi-Giunti, B., Laabir, M., Vaquer, A., 2006. The benthic resting cyst: a key actor in harmful dinoflagellate blooms-A review. Vie Milieu 56, 327–337.

Genovesi, B., Mouillot, D., Laugier, T., Fiandrino, A., Laabir, M., Vaquer, A., Grzebyk, D., 2013. Influences of sedimentation and hydrodynamics on the spatial distribution of *Alexandrium catenella/tamarense* resting cysts in a shellfish farming lagoon impacted by toxic blooms. Harmful Algae 25, 15–25.

Glibert, P.M., Burford, M.A., 2017. Globally changing nutrient loads and harmful algal blooms: recent advances, new paradigms, and continuing challenges. Oceanography 30, 58–69.

Gotelli, N.J., Ellison, A.M., 2004. Primer of Ecological Statistics. Sinauer Associates Publishers.

Gray, D.D., Zonneveld, K.A., Versteegh, G.J., 2017. Species-specific sensitivity of dinoflagellate cysts to aerobic degradation: a five-year natural exposure experiment. Rev. Palaeobot. Palynol. 247, 175–187.

Gribble, K.E., Nolan, G., Anderson, D.M., 2007. Biodiversity, biogeography and potential trophic impact of Protoperidinium spp.(Dinophyceae) off the southwestern coast of Ireland. J. Plankton Res. 29, 931–947.

Guzmán, L., Pacheco, H., Pizarro, G., Alárcon, C., 2002. *Alexandrium catenella* y veneno paralizante de los mariscos en Chile. In: Sar, E.A., Ferrario, M.E., Reguera, B. (Eds.), Floraciones Algales Nocivas en el Cono Sur Americano. Instituto Español de Oceanografía, Madrid, España, pp. 235–255.

Hallegraeff, G.M., 1992. Harmful algal blooms in the Australian region. Mar. Pollut. Bull. 25, 186–190.

Hallegraeff, G.M., 1993. A review of harmful algal blooms and their apparent global increase. Phycologia 32, 79–99.

Hallegraeff, G.M., Anderson, D.M., Belin, C., Bottein, M.-Y.D., Bresnan, E., Chinain, M., Enevoldsen, H., Iwataki, M., Karlson, B., McKenzie, C.H., 2021. Perceived global increase in algal blooms is attributable to intensified monitoring and emerging bloom impacts. Commun. Earth Environ. 2, 1–10.

Hambright, K.D., Zamor, R.M., Easton, J.D., Allison, B., 2014. Algae. In: Wexler, Philip (Ed.), Encyclopedia of Toxicology, , third ed.vol. 1. Elsevier Inc., Academic Press, pp. 130–141.

Head, M., 1996. Modern dinoflagellate cysts and their biological affinities. Palynology: Princ. Appl. 3, 1197–1248.

Heisler, J., Glibert, P.M., Burkholder, J.M., Anderson, D.M., Cochlan, W., Dennison, W. C., Dortch, Q., Gobler, C.J., Heil, C.A., Humphries, E., 2008. Eutrophication and harmful algal blooms: a scientific consensus. Harmful Algae 8, 3–13.

Hesse, K.-J., Tillmann, U., Nehring, S., Brockmann, U., 1997. Factors controlling phytoplankton distribution in coastal waters of the German Bight (North Sea). Oceanogr. Lit. Rev. 2, 114–115.

Ignatiades, L., Gotsis-Skretas, O., 2010. A review on toxic and harmful algae in Greek coastal waters (E. Mediterranean Sea). Toxins 2, 1019–1037.

Iriarte, J.L., González, H.E., Nahuelhual, L., 2010. Patagonian fjord ecosystems in southern Chile as a highly vulnerable region: problems and needs. Ambio 39, 463–466.

Jeong, H., Shim, J., Kim, J., Park, J., Lee, C., 1998. Growth and grazing rates of a thecate mixotrophic dinoflagellate *Fragilidium* cf. *mexicanum* on a red tide dinoflagellate *Lingulodinium polyedrum*. In: Reguera, B., Blanco, J., Fernández, M.L., Wyatt, T. (Eds.), Harmful Algae. Xunta de Galicia and IOC of UNESCO, pp. 179–181. Grafisant, Santiago de Compostela.

Joyce, L., Pitcher, G., Du Randt, A., Monteiro, P., 2005. Dinoflagellate cysts from surface sediments of Saldanha Bay, South Africa: an indication of the potential risk of harmful algal blooms. Harmful Algae 4, 309–318.

Keafer, B.A., Buesseler, K.O., Anderson, D.M., 1992. Burial of living dinoflagellate cysts in estuarine and nearshore sediments. Mar. Micropaleontol. 20, 147–161.

Klais, R., Tamminen, T., Kremp, A., Spilling, K., Olli, K., 2011. Decadal-scale changes of dinoflagellates and diatoms in the anomalous Baltic Sea spring bloom. PLoS One 6, e21567.

Kremp, A., 2013. Diversity of dinoflagellate life cycles: facets and implications of complex strategies. Biol. Geol. perspect. dinoflagellates 5, 197.

Kremp, A., Anderson, D.M., 2000. Factors regulating germination of resting cysts of the spring bloom dinoflagellate *Scrippsiella hangoei* from the northern Baltic Sea. J. Plankton Res. 22, 1311–1327.

Krock, B., Borel, C.M., Barrera, F., Tillmann, U., Fabro, E., Almandoz, G.O., Ferrario, M., Cardona, J.E.G., Koch, B.P., Alonso, C., 2015. Analysis of the hydrographic conditions and cyst beds in the San Jorge Gulf, Argentina, that favor dinoflagellate population development including toxigenic species and their toxins. J. Mar. Syst. 148, 86–100.

Krumbein, W.C., 1938. Size frequency distributions of sediments and the normal phi curve. J. Sediment. Res. 8, 84–90.

Kudela, R., Berdalet, E., Urban, E., 2015. Harmful Algal Blooms: A Scientific Summary for Policy Makers.

Legendre, P., Anderson, M.J., 1999. Distance-based redundancy analysis: testing multispecies responses in multifactorial ecological experiments. Ecol. Monogr. 69, 1-24.

Liu, Y., Hu, Z., Deng, Y., Tang, Y.Z., 2020a. Evidence for production of sexual resting cysts by the toxic dinoflagellate *Karenia mikimotoi* in clonal cultures and marine sediments. J. Phycol. 56, 121–134.

Liu, Y., Hu, Z., Deng, Y., Tang, Y.Z., 2020b. Evidence for resting cyst production in the cosmopolitan toxic dinoflagellate *Karlodinium veneficum* and the cyst distribution in the China seas. Harmful Algae 93, 101788.

Lundholm, N., Ribeiro, S., Andersen, T.J., Koch, T., Godhe, A., Ekelund, F., Ellegaard, M., 2011. Buried alive–germination of up to a century-old marine protist resting stages. Phycologia 50, 629–640.

Mardones, J.I., Bolch, C., Guzmán, L., Paredes, J., Varela, D., Hallegraeff, G.M., 2016. Role of resting cysts in Chilean *Alexandrium catenella* dinoflagellate blooms revisited. Harmful Algae 55, 238–249.

Matsuoka, K., Fukuyo, Y., 2000. Technical Guide for Modern Dinoflagellate Cyst Study. WESTPAC-HAB, Japan Society for the Promotion of Science, Tokyo, Japan, pp. 6–9.

Matsuoka, K., Fukuyo, Y., 2003. Taxonomy of Cysts. Manual on Harmful Marine Microalgae. UNESCO, Paris, pp. 563–592.

Matthiessen, J., de Vernal, A., Head, M., Okolodkov, Y., Zonneveld, K., Harland, R., 2005. Modem organic-walled dinoflagellate cysts in arctic marine environments and their (paleo-) environmental significance. Paläontol. Z. 79, 3–51.

McCullagh, P., Nelder, J., 1989. Generalized Linear Models, second ed. Chapman and Hall, London. Standard book on generalized linear models.

Miyazono, A., Nagai, S., Kudo, I., Tanizawa, K., 2012. Viability of *Alexandrium tamarense* cysts in the sediment of Funka Bay, Hokkaido, Japan: over a hundred year survival times for cysts. Harmful Algae 16, 81–88.

Oksanen, J., Blanchet, F., Kindt, R., Legendre, P., Minchin, P., O'Hara, R., Simpson, G., Solymos, P., Stevens, M., Wagner, H., 2018. Package 'vegan'—Community Ecology Package. 2019. View Article.

Paliy, O., Shankar, V., 2016. Application of multivariate statistical techniques in microbial ecology. Mol. Ecol. 25, 1032–1057.

Pantoja, S., Iriarte, J.L., Daneri, G., 2011. Oceanography of the Chilean Patagonia. Continent. Shelf Res. 31, 149–153.

Paz, B., Daranas, A.H., Norte, M., Riobó, P., Franco, J.M., Fernández, J.J., 2008. Yessotoxins, a group of marine polyether toxins: an overview. Mar. Drugs 6, 73–102.

Pérez-Santos, I., Garcés-Vargas, J., Schneider, W., Ross, L., Parra, S., Valle-Levinson, A., 2014. Double-diffusive layering and mixing in Patagonian fjords. Prog. Oceanogr. 129, 35–49.

Persson, A., 2000. Possible predation of cysts—a gap in the knowledge of dinoflagellate ecology? J. Plankton Res. 22, 803–809.

Pickard, G., 1971. Some physical oceanographic features of inlets of Chile. J. Fish. Board Can. 28, 1077–1106.

R Core Team, 2019. R: A Language and Environment for Statistical Computing. R Foundation for Statistical Computing, Vienna, Austria. URL. https://www.R-project.org/.

Ribeiro, S., Berge, T., Lundholm, N., Ellegaard, M., 2013. Hundred years of environmental change and phytoplankton ecophysiological variability archived in coastal sediments. PLoS One 8, e61184.

Rodrigo, C., 2006. Topografía submarina en canales de la Patagonia norte. Avances en el conocimiento oceanográfico de las aguas interiores Chilenas. Puerto Montt a cabo de Hornos 19–23.

Rodríguez-Villegas, C., Díaz, P.A., Pizarro, G., Salgado, P., Pérez-Santos, I., Díaz, M., Seguel, M., Baldrich, Á., Bravo, I., Iriarte, L., Figueroa, R.I., 2020. *Alexandrium catenella* cyst accumulation by passive and active dispersal agents: implications for the potential spreading risk in Chilean Patagonian fjords. Harmful Algae 96.

Rodríguez-Villegas, C., Díaz, P.A., Riobó, P., Rossignol, A.E., Rodríguez, F., Loures, P., Baldrich, Á.M., Varela, D., Sandoval-Sanhueza, A., Figueroa, R., 2021a. Latitudinal variation in the toxicity and sexual compatibility of Alexandrium catenella strains from southern Chile. Toxins 13, 900, 1-16.

Rodríguez-Villegas, C., Lee, M.R., Salgado, P., Figueroa, R.I., Baldrich, Á.M., Pérez-Santos, I., Tomasetti, S.J., Niklitschek, E., Díaz, M., Álvarez, G., Marín, S.L., Seguel, M., Farías, L., Díaz, P.A., 2021b. Drivers of dinoflagellate benthic cyst assemblages in the NW Patagonian fjords system and its adjacent oceanic shelf, with a focus on harmful species. Sci. Total Environ. 785, 147378.

Salgado, P., Figueroa, R.I., Ramilo, I., Bravo, I., 2017. The life history of the toxic marine dinoflagellate *Protoceratium reticulatum* (Gonyaulacales) in culture. Harmful Algae 68, 67–81.

Sampayo, M., 1998. *Polykrikos kofoidii* Chatton predation on *Gymnodinium catenatum* Graham and its effects. In: Reguera, B., Blanco, J., Fernández, M.L., Wyatt, T. (Eds.), Harmful Algae. Xunta de Galicia and IOC of UNESCO, pp. 182–183. Grafisant, Santiago de Compostela.

Satake, M., MacKenzie, L., Yasumoto, T., 1997. Identification of *Protoceratium reticulatum* as the biogenetic origin of yessotoxin. Nat. Toxins 5, 164–167.

Schlitzer, R., 2019. Ocean Data View. https://odv.awi.de.

Schneider, W., Pérez-Santos, I., Ross, L., Bravo, L., Seguel, R., Hernández, F., 2014. On the hydrography of Puyuhuapi channel, Chilean Patagonia. Prog. Oceanogr. 129, 8–18.

Seguel, M., Díaz, P.A., Labra, G., 2015. Patrones de distribución y abundancia de quistes de dinoflagelados en sedimientos recientes de la Patagonia Chilena. Revista Ciencia y Tecnología del Mar 36, 129–155.

Seguel, M., Tocornal, M.A., Sfeir, A., 2005. Floraciones algales nocivas en los canales y fiordos del sur de Chile. Cienc. Tecnol. del Mar 28, 5–13.

Shang, L., Hu, Z., Deng, Y., Liu, Y., Zhai, X., Chai, Z., Liu, X., Zhan, Z., Dobbs, F.C., Tang, Y.Z., 2019. Metagenomic sequencing identifies highly diverse assemblages of dinoflagellate cysts in sediments from ships' ballast tanks. Microorganisms 7, 250.

Shin, H.H., Yoon, Y.H., Kim, Y.-O., Matsuoka, K., 2011. Dinoflagellate cysts in surface sediments from southern coast of Korea. Estuar. Coast 34, 712–725.

Silva, N., Vargas, C.A., 2014. Hypoxia in Chilean patagonian fjords. Prog. Oceanogr. 129, 62–74.

Smayda, T.J., 1990. Novel and Nuisance Phytoplankton Blooms in the Sea: Evidence for a Global Epidemic. RWS-North Sea Directorate.

Smayda, T.J., 1997. Harmful algal blooms: their ecophysiology and general relevance to phytoplankton blooms in the sea. Limnol. Oceanogr. 42, 1137–1153.

Søndergaard, M., 2009. Redox Potential, Encyclopedia of Inland Waters. Pergamon Press, pp. 852–859.

Strub, P.T., James, C., Montecino, V., Rutllant, J.A., Blanco, J.L., 2019. Ocean circulation along the southern Chile transition region (38°–46° S): mean, seasonal and interannual variability, with a focus on 2014–2016. Prog. Oceanogr. 172, 159–198.

Tillmann, U., Elbrächter, M., Krock, B., John, U., Cembella, A., 2009. *Azadinium spinosum* gen. et sp. nov.(Dinophyceae) identified as a primary producer of azaspiracid toxins. Eur. J. Phycol. 44, 63–79.

Trainer, V.L., Davidson, K., Wakita, K., Berdalet, E., Suddleson, M., Myre, G., Trethewey, D., 2020. GlobalHAB: Evaluating, Reducing and Mitigating the Cost of Harmful Algal Blooms: A Compendium of Case Studies, vol. 28. PICES Press, pp. 30–32.

Tubaro, A., Dell'Ovo, V., Sosa, S., Florio, C., 2010. Yessotoxins: a toxicological overview. Toxicon 56, 163–172.

Van Egmond, H.P., Van Apeldoorn, M.E., Speijers, G.J.A., 2004. Marine Biotoxins. Food and Agriculture Organization of the United Nations, vol. 80. Rome, Italy.

Varela, D., Paredes, J., Alves-de-Souza, C., Seguel, M., Sfeir, A., Frangópulos, M., 2012. Intraregional variation among *Alexandrium catenella* (Dinophyceae) strains from southern Chile: morphological, toxicological and genetic diversity. Harmful Algae 15, 8–18.

Venables, W.N., Ripley, B.D., 2010. Modern Applied Statistics with S, fourth ed. Springer Publishing Company, Incorporated, New York, USA.

Venables, W.N., Ripley, B.D., 2013. Modern Applied Statistics with S-PLUS, 3th ed. Springer Science & Business Media, New York, USA.

Wasserstein, R.L., Lazar, N.A., 2016. The ASA statement on p-values: context, process, and purpose. Am. Statistician 70 (2), 129–133.

Wells, M.L., Karlson, B., Wulff, A., Kudela, R., Trick, C., Asnaghi, V., Berdalet, E., Cochlan, W., Davidson, K., De Rijcke, M., 2020. Future HAB science: directions and challenges in a changing climate. Harmful Algae 91, 101632.

Wentworth, C.K., 1922. A scale of grade and class terms for clastic sediments. J. Geol. 30, 377–392.

Yarimizu, K., Fujiyoshi, S., Kawai, M., Norambuena-Subiabre, L., Cascales, E.-K., Rilling, J.-I., Vilugrón, J., Cameron, H., Vergara, K., Morón-López, J., 2020. Protocols for monitoring harmful algal blooms for sustainable aquaculture and coastal fisheries in Chile. Int. J. Environ. Res. Publ. Health 17, 7642.

Young, N., Sharpe, R.A., Barciela, R., Nichols, G., Davidson, K., Berdalet, E., Fleming, L. E., 2020. Marine harmful algal blooms and human health: a systematic scoping review. Harmful Algae 98, 101901.

Zmerly, H., Laabir, M., Lafabrie, C., Malouche, D., Bancon-Montigni, C., González, C., Deidun, A., Pringault, O., Daly-Yahia, O., 2017. Do the levels of industrial pollutants influence the distribution and abundance of dinoflagellate cysts in the recently-deposited sediment of a Mediterranean coastal ecosystem? Sci. Total Environ. 595, 380–392.

ZoBell, C.E., 1946. Studies on redox potential of marine sediments. AAPG (Am. Assoc. Pet. Geol.) Bull. 30, 477–513.